Technical Report TE-77-7

MODELING, ANALYSIS AND SIMULATION OF TARGETS AND BACKGROUNDS FOR INFRARED SEEKERS

Advanced Sensors Directorate
Technical Information Office

April 1977

US Army Missile Research and Development Command
Redstone Arsenal, Alabama 35809

DISPOSITION INSTRUCTIONS

DESTROY THIS REPORT WHEN IT IS NO LONGER NEEDED. DO NOT RETURN IT TO THE ORIGINATOR.

DISCLAIMER

THE FINDINGS IN THIS REPORT ARE NOT TO BE CONSTRUED AS AN OFFICIAL DEPARTMENT OF THE ARMY POSITION UNLESS SO DESIGNATED BY OTHER AUTHORIZED DOCUMENTS.

TRADE NAMES

USE OF TRADE NAMES OR MANUFACTURERS IN THIS REPORT DOES NOT CONSTITUTE AN OFFICIAL INDORSEMENT OR APPROVAL OF THE USE OF SUCH COMMERCIAL HARDWARE OR SOFTWARE.

UNCLASSIFIED

SECURITY CLASSIFICATION OF THIS PAGE (When Data Entered)

REPORT DOCUMENTATION PAGE	READ INSTRUCTIONS BEFORE COMPLETING FORM
1. REPORT NUMBER: TE-77-7	2. GOVT ACCESSION NO. 9 / 3. RECIPIENT'S CATALOG NUMBER
4. TITLE (and Subtitle): MODELING, ANALYSIS AND SIMULATION OF TARGETS AND BACKGROUNDS FOR INFRARED SEEKERS.	5. TYPE OF REPORT & PERIOD COVERED
	6. PERFORMING ORG. REPORT NUMBER: TE-77-7
7. AUTHOR(s): Gene E. Gwins, H. Tracy Jackson	8. CONTRACT OR GRANT NUMBER(s)
9. PERFORMING ORGANIZATION NAME AND ADDRESS: Commander, US Army Missile Research and Development Command, Attn: DRDMI-TE, Redstone Arsenal, Alabama 35809	10. PROGRAM ELEMENT, PROJECT, TASK AREA & WORK UNIT NUMBERS: DA 1W362303A214, AMCMS 632303.2140311.05
11. CONTROLLING OFFICE NAME AND ADDRESS: Commander, US Army Missile Research and Development Command, Attn: DRDMI-TI, Redstone Arsenal, Alabama 35809	12. REPORT DATE: April 1977
	13. NUMBER OF PAGES: 81
14. MONITORING AGENCY NAME & ADDRESS (if different from Controlling Office)	15. SECURITY CLASS. (of this report): UNCLASSIFIED
	15a. DECLASSIFICATION/DOWNGRADING SCHEDULE

16. DISTRIBUTION STATEMENT (of this Report)

Approved for public release; distribution unlimited.

17. DISTRIBUTION STATEMENT (of the abstract entered in Block 20, if different from Report)

18. SUPPLEMENTARY NOTES

19. KEY WORDS (Continue on reverse side if necessary and identify by block number)

Passive infrared targets
Clutter
Surface vehicle discriminant
Acquisition techniques

20. ABSTRACT (Continue on reverse side if necessary and identify by block number)

This report is the first of an anticipated series of progress reports on target/background modeling related to the US Army Missile Research and Development Command's Ground Target Signature Program. This report contains a mathematical model of the data collection system and a generic class of seekers, plus general purpose digital computer models capable of analyzing raw thermal imagery of target-clutter data. The computer program methodology and algorithm flow

ABSTRACT (Continued)

DD FORM 1 JAN 73 1473 EDITION OF 1 NOV 65 IS OBSOLETE

UNCLASSIFIED

SECURITY CLASSIFICATION OF THIS PAGE (When Data Entered)

ABSTRACT (Concluded)

require the AGA Thermovision information in a discrete input format. Furthermore, the computer programs output results in a three dimensional plot of infrared intensity as a function of aspect angle for every object in each Thermovision data frame. A two-dimensional matrix is generated to represent infrared intensity as a function of position for 10,000 data points on each Thermovision picture. A computer generated interactive graphics plot of objects grouped by intensity produces a histogram distribution for each Thermovision data frame. Such a histogram may be used to assess the feasibility of automatic target cueing technology in detecting and recognizing tactical targets in forward looking infrared imagery.

CONTENTS

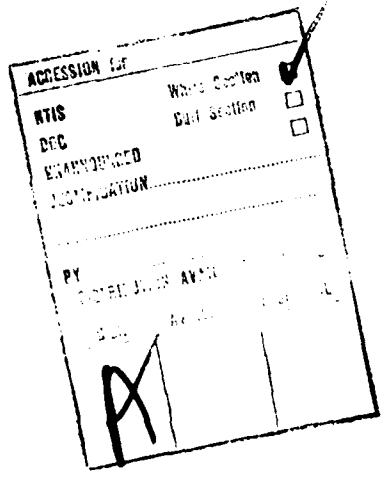

ACKNOWLEDGMENT

Appreciation is expressed to Sibley Walters, Eglin Air Force Base, for the development of the BASES computer model. The authors wish to thank Mr. Glenn Riley, Georgia Institute of Technology, for the numerous unique ideas and concepts which led to the development and application of the computer models outlined and discussed in this report. The authors acknowledge Mr. Bill Edwards, who contributed to the programming, checkout of the models, and inclusion of many features allowing compact input, output, and economical computing speed.

I. OBJECTIVE

The objectives of this program are to characterize passive infrared (IR) targets and clutter through measurements and computer analysis which would, when completed, evaluate a conceptual seeker algorithm's mathematical equivalent for effectiveness against a given threat within that threat's operational scenario. These objectives will be achieved by conducting a systematic and exhaustive search for surface vehicle target/clutter discriminants and the development of computer software to evaluate these discriminants.

II. INTRODUCTION

The US Army Missile Research and Development Command (MIRADCOM) Advanced Sensors Directorate is currently conducting a Ground Target Signatures Program to investigate and evaluate passive IR targets and background (clutter) signatures and identify potential target discrimination and acquisition techniques. The thrust and direction of this program imposes requirements that the search for discriminants be conducted in as systematic and exhaustive a manner as possible and that reliance on hit-or-miss postulation of likely discriminants be minimized.

Although a completely systematic and rigorously exhaustive approach is not presently feasible, it is possible to initiate search techniques which are systematic and exhaustive within a class of discriminants. Thus, the IR target-clutter discrimination program is being developed along two concurrent lines of inquiry:

a) A study of the physical processes involved in a seeker-clutter-target complex with a view toward gaining understanding of the signal parameters which might plausibly provide discrimination information.

b) A more innovative line, consisting of a characterization of the stochastic properties of signals emitted from targets and backgrounds of interest, in a systematic search for persistent differences in signal distributions associated with various target backgrounds classes.

Because this program deals with land vehicles, the interaction of the target with a variety of backgrounds must be utilized. The discriminants must not be based solely on the bare-body signatures of the target but on parameters of the seeker-clutter-target complex. These discriminants have many possibilities such as spectral, spatial, amplitude, or combinations of these properties of both the target and background. Therefore, the major goal is to avoid a hit-or-miss approach to the selection of discriminants. Considerable effort is being spent on the development of systematic techniques to determine a set of signature parameters that distinguish one class of objects from the other. These parameters can then be utilized to define a seeker and its acquisition and tracking algorithm to discriminate between targets and various

backgrounds. Once the seeker algorithm has been determined for a particular set of discriminants, an estimate can be made of applicability to a given threat and operational scenario.

III. PROGRAM RATIONALE

The program organization and priorities were determined by answers to two questions which were: (1) What data (in terms of scene information content) does a passive IR seeker need to operate when receiving a real tactical scene? and (2) How does one go about collecting data to duplicate a scene containing this information such that target acquisition techniques can be investigated?

Question (1) was answered by an extensive literature search at the Terminal Homing Data Bank, a review of present operational systems, and a review of the state-of-the-art in passive IR seeker programs within government and industry. These results indicate that most passive IR operational and state-of-the-art seeker systems operate on some method of spatial frequency filtering of the collected target/clutter and power contained within the filtered frequency components. Some development programs are extending these techniques to multispectral band systems with spatial frequency filtering and statistical analysis of clutter and targets.

Question (2) is answered by direct application of this program to seeker systems. This forces a consideration of both present seekers containing IR detectors with mechanical scanners and second generation Charge Transfer Devices (CTD) IR detectors. Present day seekers with mechanical scanners generate many different scan patterns including a raster format. The second generation CTD IR detectors consist primarily of matrix arrays or line arrays which are read out in a raster format. Therefore, due to the extensive work required to carry out this program, it was concluded that collection and analysis of data in a raster format would best serve the long and short range needs.

IV. PROBLEM DEFINITION

After a brief review of the voluminous literature applicable to target/clutter discrimination, it becomes obvious that a well-planned and continuous Ground Targets Signatures Program is essential if reliable seeker algorithms are to be developed at minimum cost. The present program is aligned along traditional target/clutter functional lines with separate and combinational evaluations of spectral, spatial, and temperature characteristics of targets as a function of operating conditions and environment; natural background, spatial and spectral distributions and the effects of these distributions when man-made objects are added to natural backgrounds; mathematical modeling of the sensor-target-clutter complex; and target/background discrimination signal processing techniques

applicable to seeker acquisition problems.

A significant degree of intuitive insight into the problem may be gained by taking thermograph images of a wide variety of potential target scenes, expressing these images in a digital format, reducing the corresponding digital data, and exercising a computer model to predict seeker acquisition performance. Consequently, this report will elaborate on the thermal imagery data gathering system, reducing the data and utilization of computer models to identify true target-false target problems and predict seeker acquisition performance.

V. COMPUTER FORMAT OF AGA THERMOVISION

The ability to predict the performance of any passive infrared seeker system accurately requires a model containing a realistic tactical scene including both target and background clutter, plus a realistic model of the data collection device and seeker system being considered. Furthermore, the timely assessment of the impact of seeker, target, and clutter parameter variations necessitates the codification of this model into a form amenable to quick response parametric analysis. To these ends, a mathematical model (Appendix A) has been developed to describe the data collection system and a generic class of seekers. Simultaneously with this effort, fast running computer programs have been developed to investigate collected AGA Thermovision target/clutter data statistics.

A. Data Collection System

The data collection system is a raster type scanner as described in Appendix A manufactured in Sweden by AGA AKTIEBOLAG. The system contains two major subassemblies; the camera head and an electronics control/display console. The camera head consists of a silicon lens with a 134-mm focal length and a maximum aperture opening of f/1.5. The optical system uses a variable aperture stop to control the field-of-view (FOV) and an image plane scanner designed to product a raster scan at 16 frames/sec over a 10° by 10° square FOV. The scan rate is determined by the 280 vertical line 2/1 interlace raster with 140 unambiguous data points per horizontal line and 140 unambiguous vertical line resolution capability. The single detector is an InSb photovoltaic detector operating at 77°K by means of a nitrogen dewar. The detector angular subtense for both horizontal and vertical FOV is 1.3 mrad. The scan rate and electronics frequency of this system is given in Equation (22) of Appendix A as:

$$\Delta f = \frac{\pi\, fo}{2} = \frac{\pi}{2} \left[\frac{(XFOV)\ (YFOV)\ F_R\ N_{os}}{2\ N_p\ \Delta x\ \Delta y\ N_{se}} \right]$$

where

XFOV = horizontal FOV (mrad)

= 174 mrad

YFOV = vertical FOV (mrad)

= 174 mrad

F_R = frame rate

= 16/sec

N_{os} = Overscan ratio

N_p = number of lines scanned in parallel

= 1

Δx = horizontal instantaneous FOV

= 1.3 mrad

Δy = vertical instantaneous FOV

= 1.3 mrad

N_{se} = scan efficiency (ratio of active scan to total scan)

The detected video signal is supplied to video amplifiers' circuits (to be calibrated with the model of Appendix A later in the program when frequency domain work begins) which amplify and filter the signal to drive a small cathode ray tube which generates a pictorial result. At the same time, the video signal is supplied to an analog-to-digital converter. The analog-to-digital converter presently digitizes approximately one frame per second and stores data serially on one track of a 14-track tape on an AMPEX-1300 tape recorder. Each digitized data frame consists of 140 vertical lines with 140 data points per line in a 10-bit word for each data point. This 14-track output tape, with one track of serially packed digitized Thermovision output data contains $140 \times 140 \times 10$ bits of information for each frame digitized. This information is then selected on a per frame basis and recorded on a parallel seven-track tape compatible with input data format requirements of an Army CDC-6600 digital computer. Further and more detailed descriptions of recording techniques and the reduction of Thermovision data will be addressed in the ensuing sections of this report.

The AGA Thermovision system is relatively small and may be mounted on helicopters or installed in a fixture at ground level to view a ground

target. In support of many different air defense and ground target signature applications, the system has been equipped with eight different bandpass filters. Each of these filters represents the IR bandpass of US Army or foreign system to be investigated.

B. AGA Thermovision Field Measurements.

In general, the AGA Thermovision system has been used in IR measurements of ground targets viewed from both fixed ground levels positions and aerial platforms. This system of data collection has proven to be reliable in many and varied applications. For example, this system has been used by the Air Force to record in-flight IR signatures of jet aircraft plumes. The Thermovision system was mounted in a pod on the wing of a chase plane.

For this application, the Thermovision was mounted on a helicopter to collect ground target and clutter data from various altitudes, ranges, and aspect angles. Due to the interaction between the target and ground clutter and a desire to gain more of an intuitive insight into the probblem, a large quantity of data has been taken for ground targets and clutter to look at statistics of both targets and clutter.

Data of this type, along with computer analysis, can evaluate and establish limits on seeker systems acquisition techniques which operate predominately on energy levels and spatial frequency. This type of data and computer analysis can also be used to assess the feasibility of automatic target cueing technology in detecting and recognizing tactical targets in forward looking infrared (FLIR) imaging systems.

C. Data Formatting

The purpose of this section is to outline steps required to process and reduce the raw Thermovision data to a computer compatible format. The block diagram of Figure 1 will be used to describe the required process from the point of data inception to the point of inputting reduced data to the CDC-6600 for analysis.

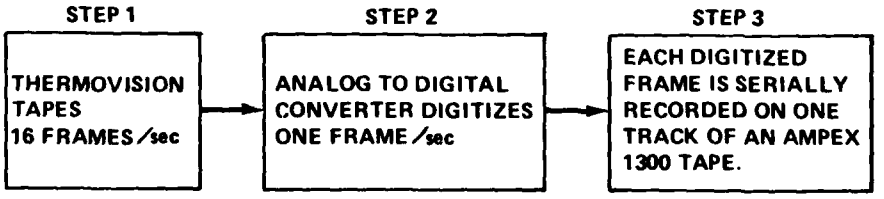

Figure 1. AGA Thermovision data recording process.

During Step 1, each Thermovision data frame is composed of 140 lines with 140 resolution elements per line; consequently, if each data point is represented with a 10-bit word ($16 \times 140 \times 140 \times 10$ bits of information), a string of 3.136×10^6 bits would require recording on magnetic tape each second. This data rate is well beyond the tape drive operating capability; therefore, an analog-to-digital converter was developed to digitize one frame per second, approximately 196,000 bits of information per frame. This requires the matching of lines from frame to frame to reconstruct one frame out of every 16 frames. To assure correct frame reconstruction, the last two data points at the end of each frame have a special coded value. Therefore, at the end of Step 3, a 14-track AMPEX-1300 tape is generated with digital Thermovision information on only one track. A physical representation of the one track is shown in Figure 2. Each line is composed of Data Point 1 (D1) through Data Point 140 (D140); each data point is represented by 10 bits.

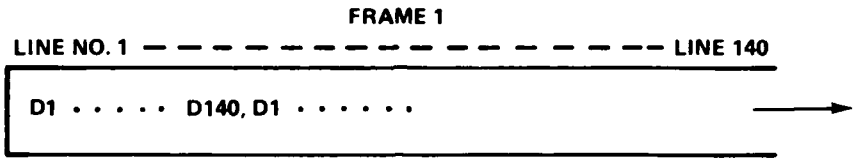

Figure 2. Data frame format.

For each line, Data Points 139 and 140 have the same special bit pattern to denote the end of a line; in addition, Data Points 139 and 140 of Line 140 are made up of a special bit pattern to identify the end of a frame. After one frame is recorded on the tape, a new frame is started; this process repeats itself until the measurements are completed or a tape is full.

Steps 4, 5, and 6 (Figure 3) are illustrated to show how the data are recorded to meet CDC-6600 input format requirements. During Step 4, a decommutator is used to select the correct coded words at the end of each line and at end of each frame to reconstruct each data frame correctly. Each frame of data is input to a PDP-15 digital computer (Step 5). During Step 6, a PDP-15 digital computer takes the serial string of bits and generates a 7-track parallel digital packed tape which may be input to a CDC-6600 computer. It must be recalled that a 10-bit word was output from the analog to digital converter to represent each 10-bit data point. This 10-bit word is now right adjusted in each of the 18-bit words output from the PDP-15 computer. Thus, at the end of Step 6, a magnetic digital tape composed of Thermovision data has been generated and is compatible with CDC-660 software.

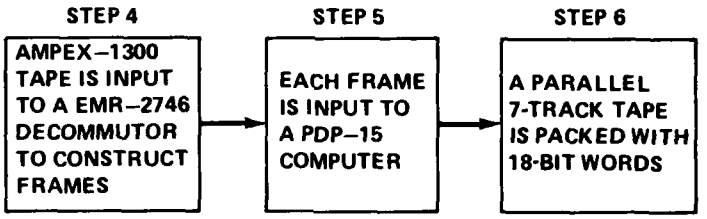

Figure 3. Data conversion to CDC-6600 format.

D. Validation of Data Format

The initial task in the Thermovision data analysis is to input to the Eglin BASES program the digital tape generated during the previously mentioned 6 steps of the data reduction process. The 10-bit input data are now contained in an 18-bit word and must be selected, sorted, and shifted into a 60-bit word. After processing through the BASES program's GETPIC routine a new 7-track parallel data tape is created, which is made up of 60-bit words, with five 12-bit words in each 60-bit word. Furthermore, the 10 bits of meaningful data are packed in each of the 12 bits of information as in the example of Figure 4.

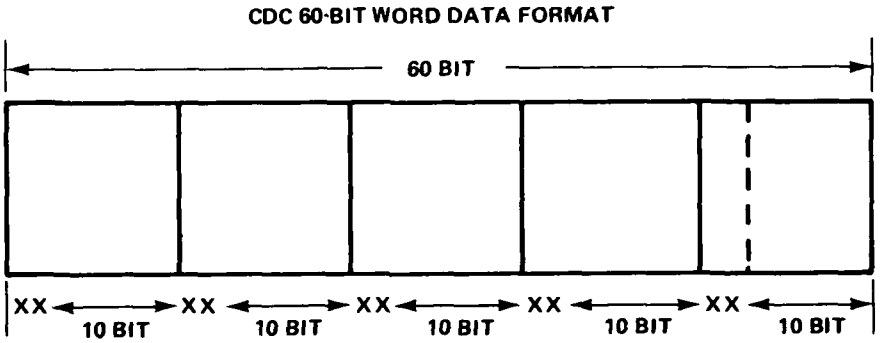

Figure 4. CDC 60-bit word data format.

After using the GETPIC routine one time to generate the new 60-bit word data tape, the BASES program may be run any number of times with the new data tape without using the GETPIC routine again. Outputs from the BASES program applied to measured data are tabulated in Table 1 for 100 of the 260 frames of data contained on the tape.

TABLE 1. EXAMPLE OUTPUT FROM BASES PROGRAM

Frame No.	Time Before Picture	Frame Time	FIL	P	GN	C L	C1 CNT	C1 LN	C1 WD	C2 CNT	C2 LN	C2 WD	MAX CNT	MAX LN	MAX WD	AVG CNT	AZ of MAX CELL	EL of MAX CELL
1	15 37 1.949	1.308	4	7	2	0	32	52	10	9	47	74	32	52	10	4	-3.571	1.159
2	15 37 3.319	1.308	4	7	2	0	32	51	7	10	51	99	32	51	7	5	-3.878	1.304
3	15 37 4.689	1.309	4	7	2	0	39	56	16	14	48	68	39	56	16	6	-2.959	.580
4	15 37 6.059	1.308	4	7	2	0	35	48	12	11	61	75	35	48	12	5	-3.367	1.739
5	15 37 7.429	1.308	4	7	2	0	39	57	18	7	46	98	39	57	18	3	-2.755	.435
6	15 37 8.800	1.308	4	7	2	0	38	42	26	7	65	88	38	42	26	4	-1.939	2.609
7	15 37 10.170	1.308	4	7	2	0	8	48	22	27	55	48	27	55	48	3	.306	.725
8	15 37 11.540	1.309	4	7	2	0	23	50	43	9	55	99	23	50	43	8	-.204	1.449
9	15 37 12.910	1.309	4	7	2	0	15	49	35	7	70	100	15	49	35	6	-1.020	1.594
10	15 37 14.280	1.308	4	7	2	0	7	53	38	7	68	97	7	89	98	5	5.408	-4.203
11	15 37 15.651	1.308	4	7	2	0	7	64	44	7	45	93	7	23	100	5	5.612	5.362
12	15 37 17.021	1.308	4	7	2	0	7	51	38	7	56	85	7	22	96	4	5.204	5.507
13	15 37 18.391	1.309	4	7	2	0	7	52	32	6	44	86	7	18	87	4	2.245	6.087
14	15 37 19.762	1.308	4	7	2	0	6	50	40	7	65	58	8	93	15	4	-3.061	-4.783
15	15 37 21.131	1.309	4	7	2	0	7	46	30	6	57	98	7	79	99	4	5.519	-2.754
16	15 37 22.502	1.308	4	7	2	0	7	54	29	7	69	91	7	91	98	4	5.408	-4.493
17	15 37 23.872	1.308	4	7	2	0	6	59	33	6	58	96	7	37	54	3	.918	3.333
18	15 37 25.242	1.309	4	7	2	0	4	62	20	4	43	99	6	21	76	2	3.163	5.652
19	15 37 26.613	1.308	4	7	2	0	7	64	45	7	67	100	7	86	100	6	5.612	-3.768
20	15 37 27.983	1.308	4	7	2	0	7	64	45	7	58	96	7	27	100	5	5.612	4.783
21	15 37 29.353	1.309	4	7	2	0	7	53	45	7	67	100	7	90	100	6	5.612	-4.348
22	15 37 30.723	1.309	4	7	2	0	7	61	45	7	63	100	7	96	100	6	5.612	-5.217
23	15 37 32.093	1.309	4	7	2	0	10	59	33	11	60	97	14	13	1	6	-4.490	6.812
24	15 37 33.464	1.308	4	7	2	0	10	63	12	12	44	47	12	44	47	5	.204	2.319
25	15 37 34.834	1.308	4	7	2	0	11	45	29	9	64	53	12	31	51	6	.612	4.203
26	15 37 36.205	1.308	4	7	2	0	10	43	41	10	54	87	10	99	47	7	.204	-5.652
27	15 37 37.574	1.309	4	7	2	0	11	64	32	15	54	75	16	23	2	6	-4.388	5.362
28	15 37 38.944	1.309	4	7	2	0	7	5	45	9	47	91	9	47	91	5	4.694	1.884
29	15 37 40.314	1.309	4	7	2	0	7	40	45	11	56	59	11	27	100	5	5.612	4.783
30	15 37 41.684	1.308	4	7	2	0	11	63	38	11	56	64	16	31	14	6	-3.163	4.203
31	15 37 43.054	1.308	4	7	2	0	11	60	7	11	50	100	11	50	100	5	5.612	1.449
32	15 37 44.424	1.309	4	7	2	0	8	65	29	9	45	62	11	92	33	5	-1.224	-4.638
33	15 37 45.795	1.308	4	7	2	0	9	56	28	11	63	69	11	86	69	6	2.449	-3.768
34	15 37 47.164	1.308	4	7	2	0	11	61	15	8	44	73	11	61	15	5	-3.061	-.145
35	15 38 54.303	1.309	4	7	2	0	9	67	37	9	47	98	39	34	8	6	-3.776	3.768
36	15 38 55.673	1.308	4	7	2	0	64	68	31	13	59	47	64	68	31	6	-1.429	-1.159
37	15 38 57.044	1.308	4	7	2	0	64	47	32	11	50	53	64	47	32	5	-1.327	1.884
38	15 38 58.414	1.308	4	7	2	0	64	45	35	7	51	94	64	45	35	3	-1.020	2.174
39	15 38 59.784	1.309	4	7	2	0	64	50	37	8	57	69	64	50	37	3	-.816	1.449
40	15 39 1.154	1.308	4	7	2	0	54	52	41	10	53	100	54	52	41	5	-.408	1.159
41	15 39 2.524	1.308	4	7	2	0	47	52	29	13	53	69	47	52	29	8	-1.633	1.159
42	15 39 3.895	1.345	4	7	2	0	39	54	40	11	47	73	39	54	40	5	-.510	.870
43	15 39 5.634	1.309	4	7	2	0	15	50	36	16	48	78	16	48	78	6	3.367	1.739
44	15 39 8.004	1.309	4	7	2	0	16	59	16	16	43	63	16	84	77	6	3.265	-3.478
45	15 39 9.374	1.308	4	7	2	0	9	56	39	11	55	78	11	55	78	5	3.367	.725
46	15 39 10.745	4.048	4	7	2	0	7	62	39	7	67	96	7	98	96	5	5.204	-5.507
47	15 39 14.854	1.309	4	7	2	0	5	48	13	6	59	96	7	25	61	3	1.633	5.072
48	15 39 16.224	1.309	4	7	2	0	7	64	45	7	69	100	7	69	100	5	5.612	-1.304
49	15 39 17.595	1.308	4	7	2	0	6	59	42	7	70	95	7	30	99	4	5.510	4.348
50	15 39 18.965	1.308	4	7	2	0	5	40	7	6	41	96	6	41	96	3	5.204	2.754

TABLE 1. EXAMPLE OUTPUT FROM BASES PROGRAM (Concluded)

Frame No.	Time Before Picture	Frame Time	FIL	P	G.	C L	C1 CNT	C1 LN	C1 WD	C2 CNT	C2 LN	C2 WD	MAX CNT	MAX LN	MAX WD	AVG CNT	AZ of MAX CELL	EL of MAX CELL
51	15 39 20.334	1.308	4	7	2	0	5	42	20	3	70	100	6	84	26	2	-1.939	-3.478
52	15 39 21.705	1.308	4	7	2	0	7	58	33	7	57	96	7	57	96	4	5.204	.435
53	15 39 23.075	1.308	4	7	2	0	7	62	45	7	40	99	8	100	27	5	-1.837	-5.797
54	15 39 24.445	1.308	4	7	2	0	7	63	45	7	57	100	8	91	98	5	5.408	-4.493
55	15 39 25.815	1.308	4	7	2	0	7	59	45	7	55	99	7	71	99	5	5.510	-1.594
56	15 39 27.185	1.308	4	7	2	0	7	69	45	7	69	100	7	76	100	5	5.612	-2.319
57	15 39 28.556	1.308	4	7	2	0	7	44	44	7	51	93	8	101	6	5	-3.980	-5.942
58	15 39 29.925	1.309	4	7	2	0	7	52	45	7	59	99	8	77	45	6	0.000	-2.464
59	15 39 31.295	1.309	4	7	2	0	4	62	12	6	59	86	7	101	8	3	-3.776	-5.942
60	15 39 32.666	1.308	4	7	2	0	7	65	45	7	45	100	7	93	100	6	5.612	-4.783
61	15 39 34.035	1.308	4	7	2	0	7	59	43	7	50	100	7	50	100	5	5.612	1.449
62	15 39 35.406	1.308	4	7	2	0	7	57	45	7	61	100	7	96	100	5	5.612	-5.217
63	15 39 36.776	1.308	4	7	2	0	7	63	45	7	67	96	7	93	100	4	5.612	-4.783
64	15 39 38.146	1.309	4	7	2	0	7	66	45	7	63	96	7	86	100	5	5.612	-3.768
65	15 39 39.516	1.308	4	7	2	0	6	56	32	6	61	88	7	89	96	3	5.204	-4.203
66	15 39 40.886	1.308	4	7	2	0	7	62	45	7	64	100	7	98	100	6	5.612	-5.507
67	15 39 42.256	1.308	4	7	2	0	6	45	2	6	47	96	7	13	96	3	5.204	6.812
68	15 41 20.903	1.308	4	7	2	0	11	66	7	9	65	96	35	35	34	9	-1.122	3.623
69	15 41 22.272	1.309	4	7	2	0	35	45	45	32	45	46	35	45	45	5	0.000	2.174
70	15 41 23.643	1.308	4	7	2	0	175	42	45	256	41	48	256	41	48	11	.306	2.754
71	15 41 25.013	15.009	4	7	2	0	18	43	1	7	44	55	18	43	1	3	-4.490	2.464
72	15 41 40.083	1.309	4	7	2	0	11	63	2	7	69	100	11	63	2	4	-4.388	-.435
73	15 41 41.454	1.308	4	7	2	0	7	69	45	7	66	97	7	87	100	3	5.612	-3.913
74	15 41 42.823	1.308	4	7	2	0	7	59	16	7	68	75	8	100	77	3	3.265	-5.797
75	15 41 44.194	1.308	4	7	2	0	7	60	2	6	42	91	7	60	2	3	-4.388	0.000
76	15 41 45.564	1.308	4	7	2	0	7	58	35	7	64	72	7	64	72	5	2.755	-.580
77	15 41 46.934	1.308	4	7	2	0	7	68	16	7	49	96	7	49	96	5	5.204	1.594
78	15 41 48.304	1.308	4	7	2	0	7	46	43	7	70	100	7	70	100	5	5.612	-1.449
79	15 41 49.674	1.308	4	7	2	0	7	49	44	7	66	96	7	66	96	5	5.204	-.870
80	15 41 51.044	1.308	4	7	2	0	7	53	45	7	67	94	7	67	94	5	5.000	-1.014
81	15 41 52.414	1.308	4	7	2	0	7	57	45	7	42	79	7	87	100	5	5.612	-3.913
82	15 41 53.784	1.309	4	7	2	0	11	70	5	7	51	100	11	71	8	5	-3.776	-1.594
83	15 41 55.154	1.308	4	7	2	0	11	70	1	7	46	97	19	72	2	5	-3.878	-1.739
84	15 41 56.524	1.308	4	7	2	0	35	70	1	7	67	100	35	70	1	6	-4.490	-1.449
85	15 41 57.895	1.308	4	7	2	0	7	70	45	7	69	95	64	76	3	7	-4.286	-2.319
86	15 41 59.264	1.308	4	7	2	0	7	69	45	7	69	100	95	81	1	7	-4.490	-3.043
87	15 42 .634	1.309	4	7	2	0	11	70	22	7	69	100	111	79	18	8	-2.755	-2.754
88	15 42 2.005	1.308	4	7	2	0	157	61	10	71	63	46	157	61	10	13	-3.571	-.145
89	15 42 3.374	1.308	4	7	2	0	17	68	2	12	69	56	175	80	7	15	-3.878	-2.899
90	15 42 4.745	1.308	4	7	2	0	236	62	1	128	65	54	236	62	1	12	-4.490	-.290
91	15 42 6.115	1.308	4	7	2	0	608	59	13	206	62	49	608	59	13	13	-3.265	.145
92	15 42 7.484	1.308	4	7	2	0	547	70	12	95	70	47	547	70	12	12	-3.367	-1.449
93	15 42 8.854	1.309	4	7	2	0	400	70	12	39	70	48	504	72	11	11	-3.469	-1.739
94	15 42 11.594	1.309	4	7	2	0	444	65	25	239	67	51	444	65	25	13	-2.041	-.725
95	15 42 12.965	1.308	4	7	2	0	336	50	20	239	52	47	336	50	20	15	-2.551	1.449
96	15 42 14.334	1.308	4	7	2	0	340	62	30	223	61	57	340	62	30	11	-1.531	-.290
97	15 42 15.704	1.309	4	7	2	0	324	67	25	202	70	53	324	67	25	11	-2.041	-1.014
98	15 42 17.075	1.308	4	7	2	0	7	70	45	7	69	100	213	88	29	10	-1.633	-4.058
99	15 42 18.444	1.308	4	7	2	0	19	70	45	19	70	50	281	82	40	10	-.510	-3.188
100	15 42 19.815	1.308	4	7	2	0	11	70	45	19	70	76	272	80	41	8	1.633	-2.899

VI. DATA INTERROGATION BY COMPUTER MODELS

In the last few years, image data processing by digital computers has become a topic of great interest, both from a practical and a theoretical standpoint. Raster format data sources are common in several applications of military technology and human analysis has proven to be totally inadequate, especially when objective information is to be extracted from large masses of data. On the other hand, the application of digital computers to mechanize raster format data analysis is far from being a straightforward implementation; computers of today, when they "see" a raster format image through an appended input unit, can at best be compared to a blind human probing the environment with a single finger. This relative clumsiness of the computer when applied to a discrimination task imposes severe constraints on processing algorithms, which must often trade elegance and generality for effectiveness. There exists today, however, a number of methods or techniques which are sufficiently general to make their dissemination across the boundaries of application areas worthwhile. Consequently, the lack of a complete theory of perception by computer has not prevented attempts to solve more complex problems such as target-clutter discrimination. This problem, as well as many other machine perceptual problems, involves pattern classification — the assignment of a physical object or event to one of several perspective categories. Extensive study of classification problems has led to an abstract mathematical model that provides the theoretical basis for classifier design. In any specific application, one must ultimately come to grips with the special characteristics of the problem at hand, such as target-clutter discrimination and target acquisition. Henceforth, the purpose of this report and others to follow on the Ground Target Signatures Program will be to give a systematic account of those principles of pattern classification and those techniques of data analysis that seem to have the widest applicability and interest to target acquisition.

A. Data Classification Model

Classification models used in present Ground Target Signatures work to be described later contain many of the elements of the most commonly used abstract models for target-clutter discrimination, the classification model. This model contains three parts: a transducer, a feature extractor, and a classifier (Figure 5). This classifier model is an approach which uses a flexible combination of both heueristic and statistical means to select and/or evaluate an optimal target-clutter discrimination system. Extensive reviews and detailed descriptions of the classifier model and other pattern recognition systems are available in the literature. The authors will here recap a general outline of the model using examples and illustrations to allow the reader to become familiar with the working concepts of pattern recognition as being applied to target-clutter discrimination in this program.

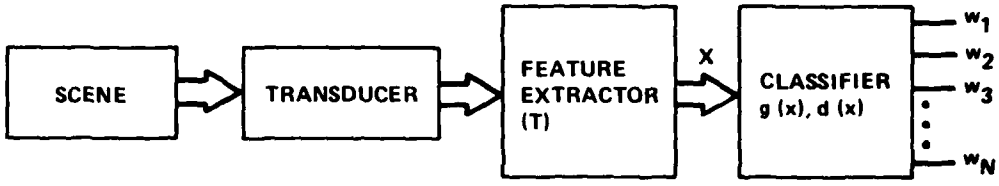

Figure 5. The classifier model.

The transducer essentially defines the observation set. That is, the transducer senses or measures the external environment and converts that information into a machine usable form. In mathematical terms, the transducer generates a p-dimensional observation vector, $y = \{Y_1, Y_2, Y_3, \ldots, Y_p\}$ where the Y_i can be any observation (amplitude, phase, frequency, physical dimensions, etc.). For this program, the transducer is the AGA Thermovision system as described earlier and generates two variables: amplitude and spatial frequency in cycles/milliradian. A third variable which is inherent in the spatial frequency content is object size provided that the range to the object is known.

The feature extractor acts on the observation to extract potentially useful information to be used by the classifier. This can be represented mathematically by Equation (1) which maps the observation vector $\bar{Y}$ into the feature vector $\bar{X}$ through the transformation, T.

$$\bar{X} = T(\bar{Y}) \tag{1}$$

There are three criteria for the optimum performance of a feature extractor: maximum separability of classes in feature space, minimum loss of discrimination information, and maximum reduction of data volume. Each of these criteria will carry different priorities according to the problem addressed and the available facilities. In general, when considering seeker systems, the highest priority will be given to maximum reduction of data to minimize the number of calculations which in turn reduces the electronics size and weight.

The classifier is used to partition the feature space into decision regions and classify each feature vector $\bar{X}$, corresponding to a set of observations as belonging to a particular class of objects (W_i). This can be thought of as another mapping, this time from the feature space, X, to the class space, C, which is a discrete space with each point representing a particular class.

The power of the classifier model is that given a set of observations, certain knowledge of the sample statistics (either calculated,

measured, or assumed) and a feature extraction procedure, the model can describe the statistical discriminatory ability of a system. The model can also be used to optimize the feature extraction process when the features have not already been determined by the type of transducer. The classifier can also be used to evaluate existing systems for performance under novel conditions. A generalized description of this total classification model is contained in Appendix B.

B. Feature Extraction by Computer Models

To illustrate the classification technique, an example problem will be used which shows some of the progress being made on this program. The example used here is a tank in a low clutter background with one other man-made object contained within the sensor FOV. A three-diminsional power plot of this scene is shown in Figure 6 which is an output from the BASES program. As defined previously, the sensor is an AGA Thermovision which produces two features (irradiance level at its optical aperture and spatial frequency in cycles/milliradian). These features (or more precisely, the value of these features) are then passed to the classifier that evaluates the evidence presented and makes a final decision as to what is target and what is clutter.

Traditionally, two features (amplitude and spatial frequency) have been used to design seeker systems. Some form of spatial frequency filtering is implemented in the form of reticles, electronic filters, etc.; the classifier then becomes a threshold detector whose level is set proportional to the scene average value. Anything that passes the spatial frequency filter and is above threshold is classified as a target. To describe this in another way, it is assumed that the seeker acquisition system has a spatial frequency bandpass similar to the AGA Thermovision. Then irradiance from the target and clutter become obvious features, and an attempt might be made to classify the target and clutter by determining if the target irradiance level measured as a voltage (V) exceeds some critical value (V_o). To choose V_o, many sample measurements, of targets at various aspect angles, altitudes, and clutter conditions may be made and a statistical analysis run on the results. This has been done; a histogram of the example scene is shown in Figure 7. When several of these histograms are accumulated, a plot similar to Figure 8 results. The accumulative histogram will or will not bear out the feasibility of a single spectrum amplitude and spatial filtering concept of seeker acquisition. The meaning of Figure 8 can be interpreted as follows: for any signal voltage level above V_1, the probability of defining a true target as target is one. This is illustrated by Figure 8 which shows the number of points and the magnitude of these points. Obviously a voltage level setting can be set for this situation but it is the total of these plots that will ultimately define the probability of success for this type of seeker processing. From Figure 8, it can be seen that if V_1 is set as shown, some loss function

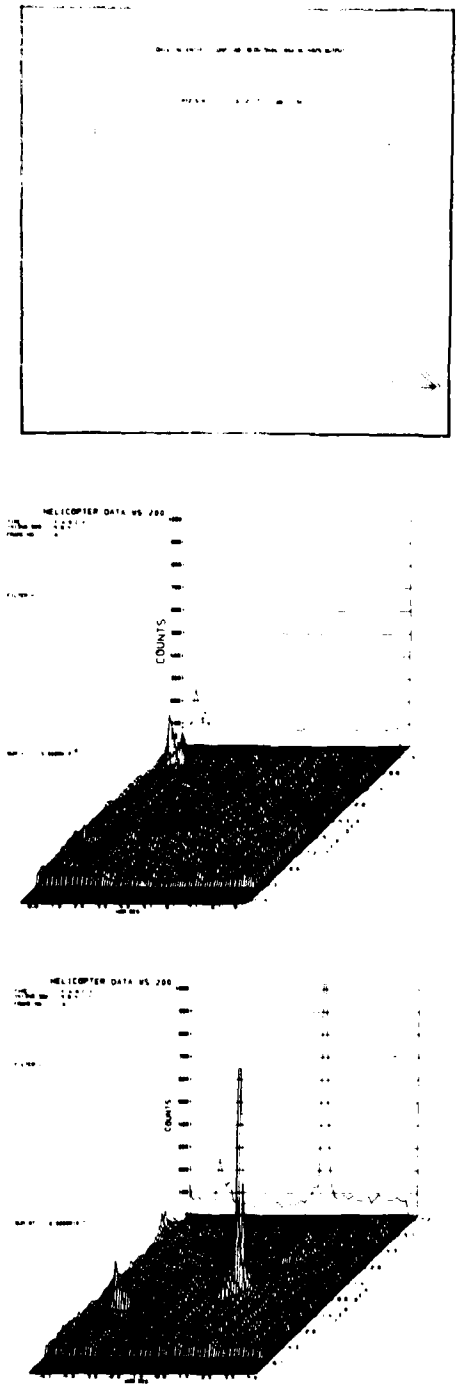

Figure 6. Three-dimensional power plot of example scene (BASES program output).

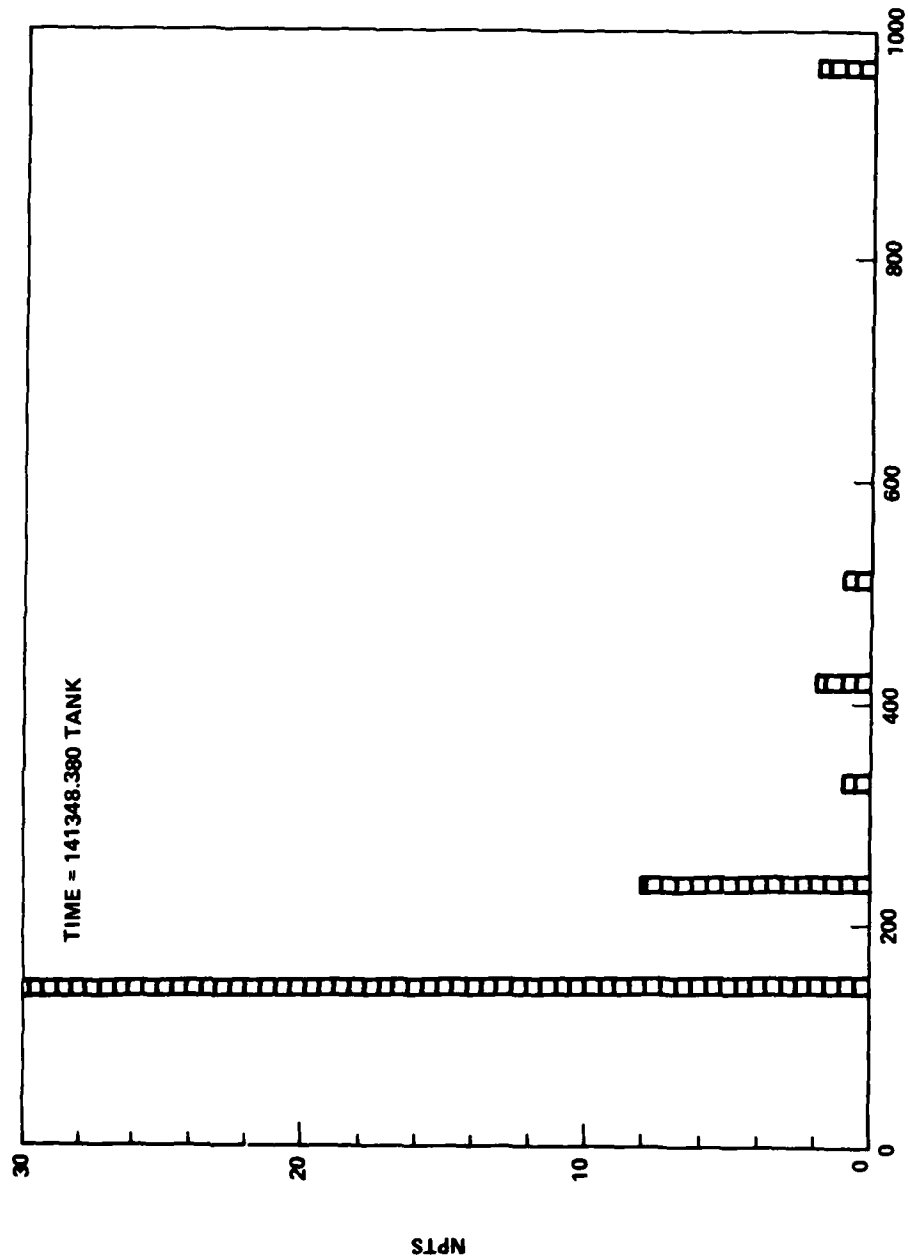

Figure 7. Histogram of example scene.

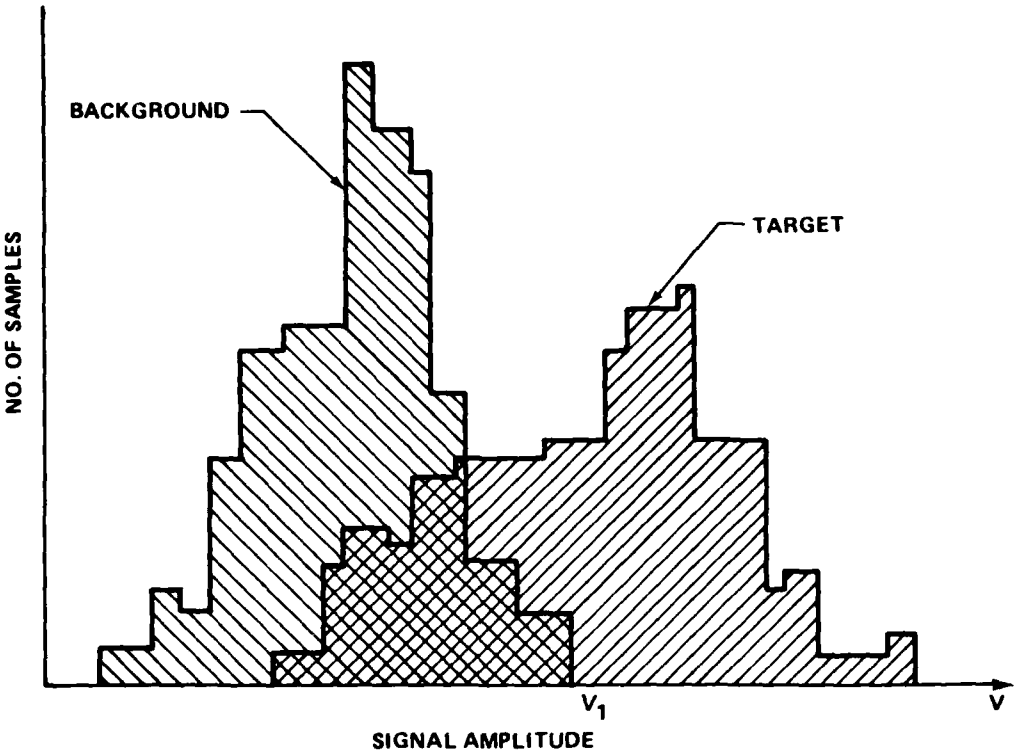

Figure 8. Statistical distributions of measurements.

will be incurred. The shaded area where target/background energy levels overlap will result in a direct loss of those targets. If V_1 is set to a lower value, then clutter will be classified as target. A sufficient amount of data exists and is being reduced to determine the exact shape of a real world curve similar to Figure 8. An alternate but similar method of presenting these data is shown in Figures 9 through 13. Figure 9 is a Versitec plot of a COMTAL display which shows the scene and runs histograms of Cursor-located fields shown as dark lines around the located field. The histograms which are plotted on the display with the scene are uncalibrated and used for operator interaction to investigate the distribution and desired field within a scene. Figures 10, 11, 12, and 13 are examples of Cursor located field histograms. Headers at the beginning of each plot show the number of points contained within the Cursor-located field and statistics of those points as well as the plot scale factors. In addition to the plot scale factors, two columns of numbers at the bottom show the energy level and the actual count at a particular energy level. Figure 10 is a plot of most of the scene as shown by the dark lines around the outside to indicate the Cursor-located field. These data represent identical data used for Figure 6 with one exception: the two least significant bits of the 10-bit words have been

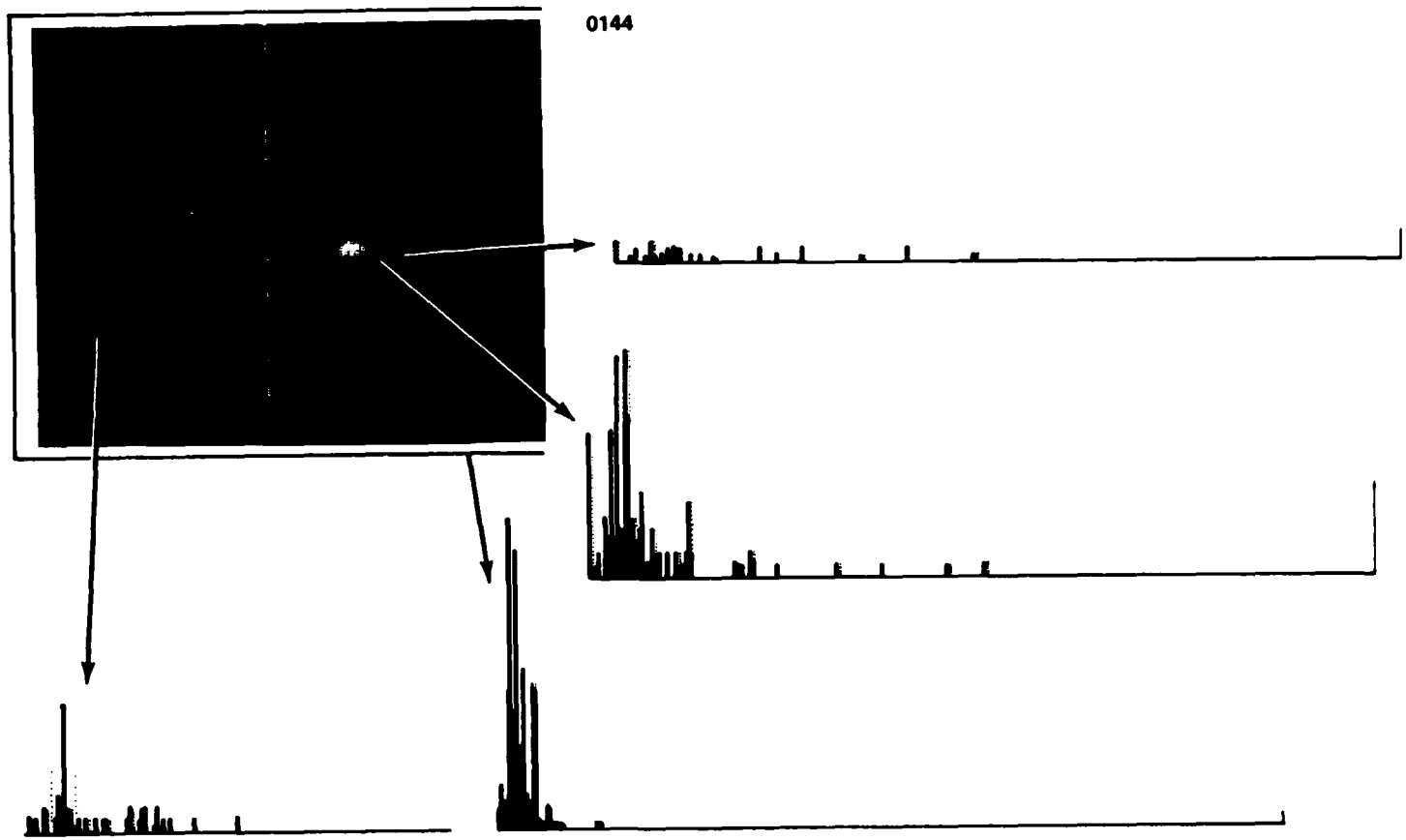

Figure 9. Low clutter scene with tank
and one other man-made object (car).

```
                                    EACH 'X' REPRESENTS    42.16 DATA POINTS
                                    HISTOGRAM TOTAL DATA POINTS=    22188.000

                                    ANALYZED INTERVAL FROM   0 TO 255
                                    MEAN--  10  MODE--   5  MEDIAN--   8
                                    STANDARD DEVIATION=  20  AVERAGE DEVIATION=  5.0
  0      269. XXXXXX
  1      540. XXXXXXXXXXXX
  2      351. XXXXXXXX
  3      312. XXXXXXX
  4     1838. XXXXXXXXXXXXXXXXXXXXXXXXXXXXXXXXXXXXXXXXXXX
  5     4216. XXXXXXXXXXXXXXXXXXXXXXXXXXXXXXXXXXXXXXXXXXXXXXXXXXXXXXXXXXXXXXXXXXXXXXXXXXXXXXXXXXXXXXXXXXXXXXXXXXXX
  6     1651. XXXXXXXXXXXXXXXXXXXXXXXXXXXXXXXXXXXXXXX
  7     3820. XXXXXXXXXXXXXXXXXXXXXXXXXXXXXXXXXXXXXXXXXXXXXXXXXXXXXXXXXXXXXXXXXXXXXXXXXXXXXXXXXXXXXXXXXX
  8     1117. XXXXXXXXXXXXXXXXXXXXXXXXXX
  9     2294. XXXXXXXXXXXXXXXXXXXXXXXXXXXXXXXXXXXXXXXXXXXXXXXXXXXXXX
 10      460. XXXXXXXXXX
 11      348. XXXXXXXX
 12     1809. XXXXXXXXXXXXXXXXXXXXXXXXXXXXXXXXXXXXXXXXXX
 13     1798. XXXXXXXXXXXXXXXXXXXXXXXXXXXXXXXXXXXXXXXXXX
 14      128. XXX
 15       96. XX
 16      349. XXXXXXXX
 17      290. XXXXXX
 18       52. X
 19       32.
 20       53. X
 21       40.
 22       12.
 23       20.
 24        0.
 25        8.
 26        0.
 27        4.
 28       16.
 29        0.
 30        4.
 31       12.
 32       32.
 33       16.
 34        0.
 35        0.
 36        0.
 37        8.
 38        0.
 39        4.
 40        0.
 41        4.
 42        0.
 43        0.
 44        0.
 45        0.
 46        0.
 47        4.
 48        4.
 49        4.
 50        0.
 51        0.
 52        8.
 53        4.
 54        0.
 55        0.
 56        0.
 57        0.
 58        0
 59        0
 60        0.
 61        4.
 62        0.
 63        4.
 64        0.


247        0.
248        0.
249        0.
250        0.
251        0.
252        0.
253        0.
254        0.
255      137. XXX
```

Figure 10. Histogram and statistics of scene in Figure 9.

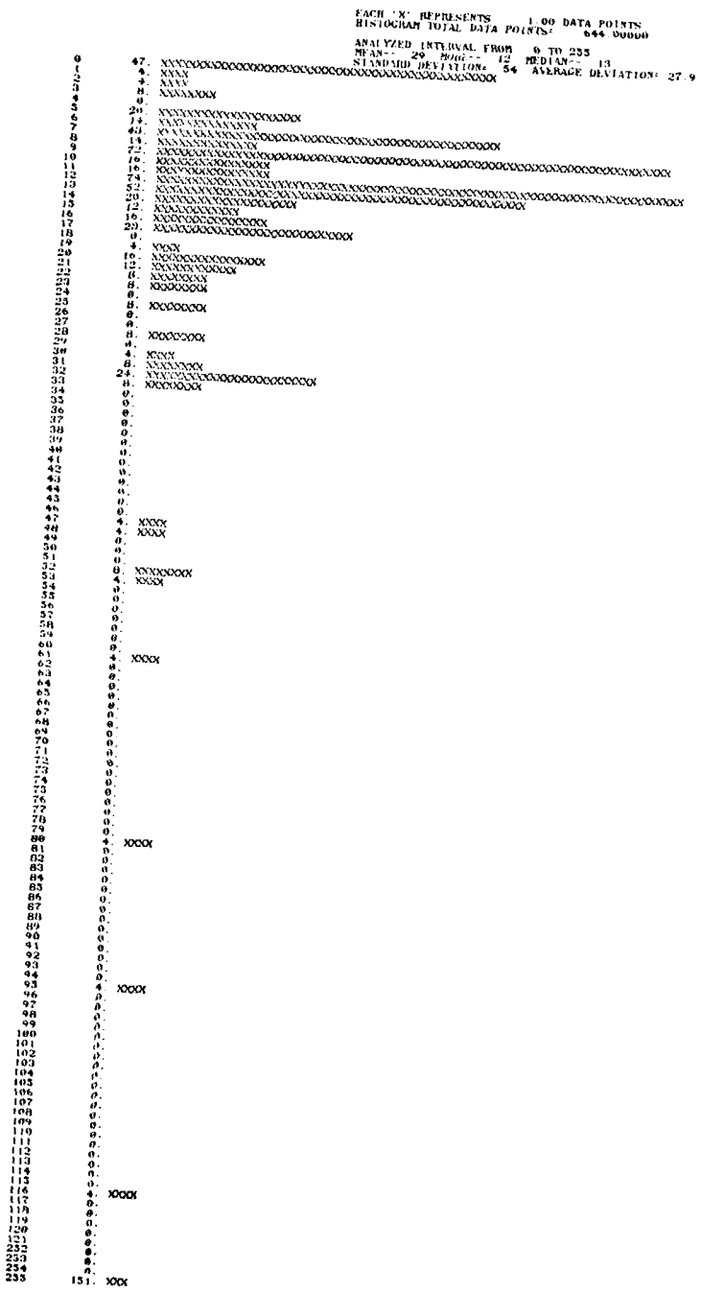

Figure 11. Histogram of large cursor located field around the target.

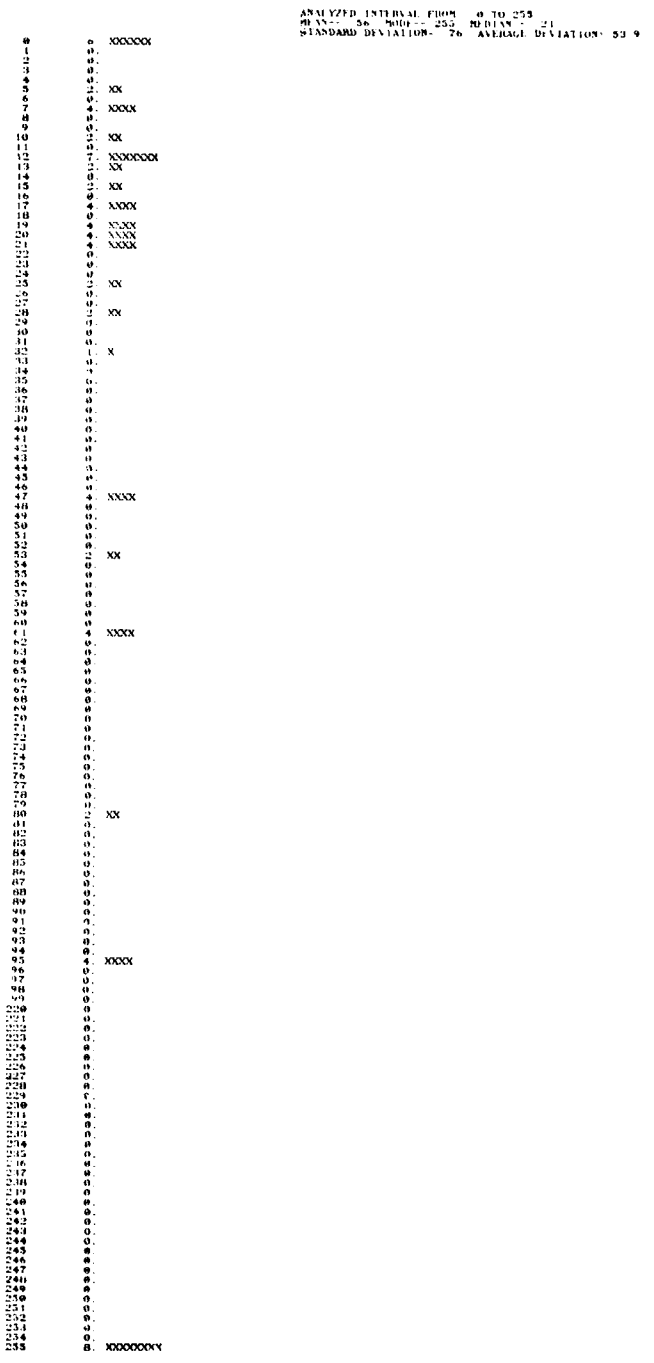

Figure 12. Histogram of cursor located field immediately surrounding the target.

```
                                    EACH 'X' REPRESENTS      1.00 DATA POINTS
                                    HISTOGRAM TOTAL DATA POINTS=     160.00000

                                    ANALYZED INTERVAL FROM   0 TO 255
                                    MEAN--  19   MODE--    7   MEDIAN--   12
                                    STANDARD DEVIATION=  15  AVERAGE DEVIATION= 12.9
  0      8. XXXXXXXX
  1      0.
  2      0.
  3      0.
  4      4. XXXX
  5     12. XXXXXXXXXXXX
  6      0.
  7     42. XXXXXXXXXXXXXXXXXXXXXXXXXXXXXXXXXXXXXXXXXX
  8      8. XXXXXXXX
  9      4. XXXX
 10      2. XX
 11      4. XXXX
 12      0.
 13      4. XXXX
 14      4. XXXX
 15      0.
 16      0.
 17      4. XXXX
 18      0.
 19      4. XXXX
 20      4. XXXX
 21      0.
 22      0.
 23      0.
 24      0.
 25      0.
 26      0.
 27      4. XXXX
 28      8. XXXXXXXX
 29      0.
 30      0.
 31      4. XXXX
 32      7. XXXXXXX
 33      8. XXXXXXXX
 34      0.
 35      0.
 36      1. X
 37      8. XXXXXXXX
 38      0.
 39      4. XXXX
 40      0.
 41      4. XXXX
 42      0.
 43      0.
 44      0.
 45      0.
 46      0.
 47      0.
 48      0.
 49      4. XXXX
 50      0.
 51      0.
 52      0.
 53      0.
 54      0.
 55      0.
 56      0.
 57      0.
 58      0.
 59      0.
 60      0.
 61      0.
 62      0.
 63      4. XXXX
 64      0.
245      0.
246      0.
247      0.
248      0.
249      0.
250      0.
251      0.
252      0.
253      0.
254      0.
255     31. XXXXXXXXXXXXXXXXXXXXXXXXXXXXXXX
```

Figure 13. Histogram of cursor located field around man-made object in scene (car).

dropped. When using these eight bits in the 22,188 data points, only 269 points showed up as zeros which again validates the data collection format. Figures 11, 12, and 13 represent histograms of a large area around the target, the target, and the other man-made objects in the scene, respectively.

C. Threshold Detection Using Histograms

Figure 14 is the output of a subroutine which uses the histograms to set thresholds and then scans the 100 × 100 data block in 10 × 10 pixel arrays. This is an example of a single scene and indicates that in this scene the true target would have been selected. However, Figure 8 shows the statistical distribution of a large number of scenes and will ultimately determine if the true target could have been selected. Further discussions of these effects and target statistics will be discussed in a later report.

VII. SUMMARY

In summary, the discriminants investigated here are the spatial radiance of target and clutter. These physical characteristics indicate (Figure 8) the probability of success of acquiring a target by effectively running a histogram and selecting a threshold based on the acquisition scene energy distribution. The overlapping areas between target and clutter represent a loss function where targets would be classified as clutter or vice versa. In the search for other features, to minimize this loss function, the most obvious step is to consider the frequency distribution of the data collected.

Figure 15 shows a three-dimensional power plot of the example scene used throughout this report. Figure 15 indicates that the target frequency content is much higher than most of the clutter. Therefore, it appears obvious that if the data set used to generate Figure 8 were broken down into frequency components, a new set of curves could be generated as a function of frequency and show the optimum frequency band for that particular set of data. For this particular set of data, with 100 × 100 resolution elements, 50 discrete frequency components with units of cycles/milliradian are contained within the scene. The distribution of these frequency components is shown in Figure 16 which is the autocorrelation function in the frequency domain. It is not obvious from this set of plots where the target energy is contained within the frequency spectrum. It becomes obvious from looking at Figures 15 and 16 that the target represents a small portion of the scene total energy. Therefore, it also becomes obvious that the dc frequency component and others of lower frequencies up to approximately one tenth of the scene should be filtered out. This would allow a target extent from 2 to 10 pixels. This would have the effect of allowing the target energy to represent a greater portion of the scene energy. From these results,

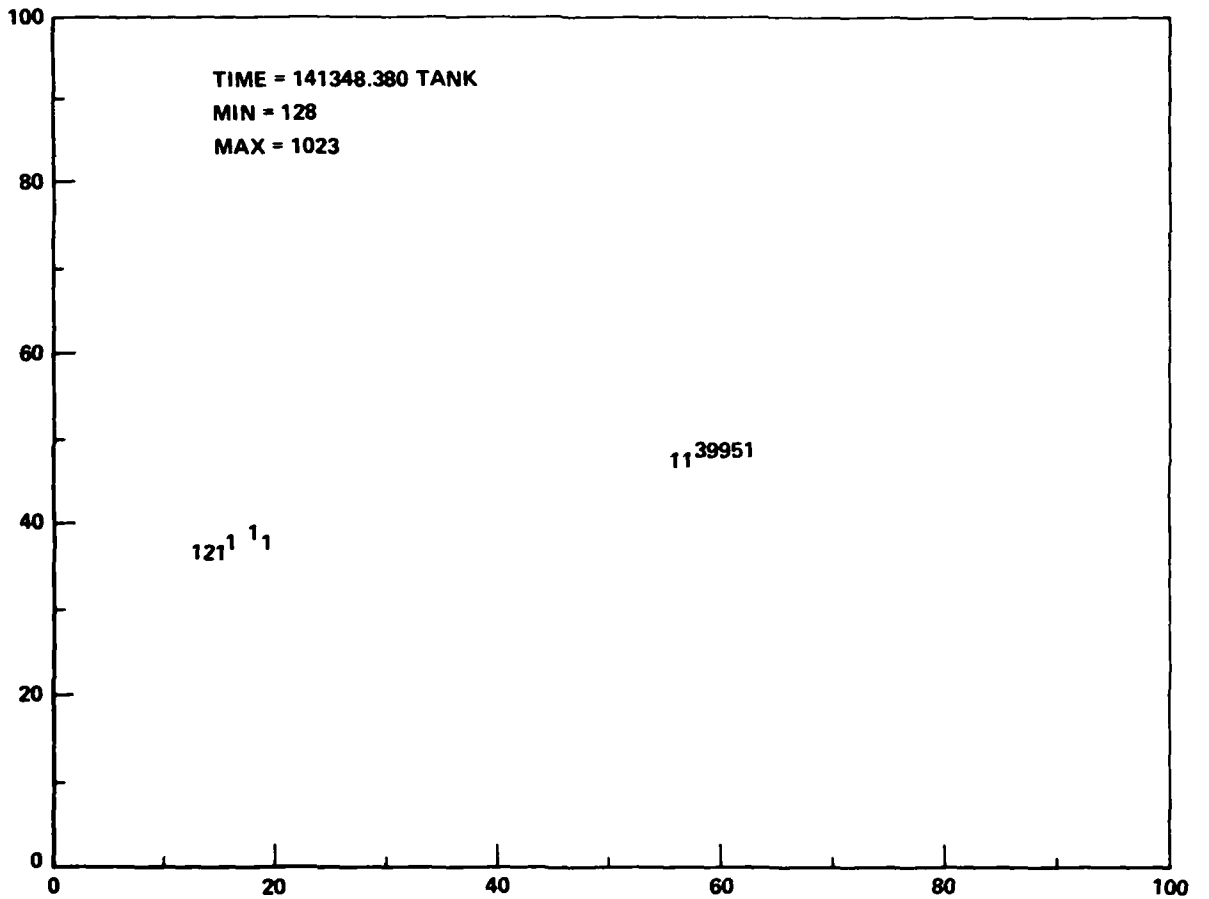

Figure 14. Threshold detection output of subroutine HSPOT.

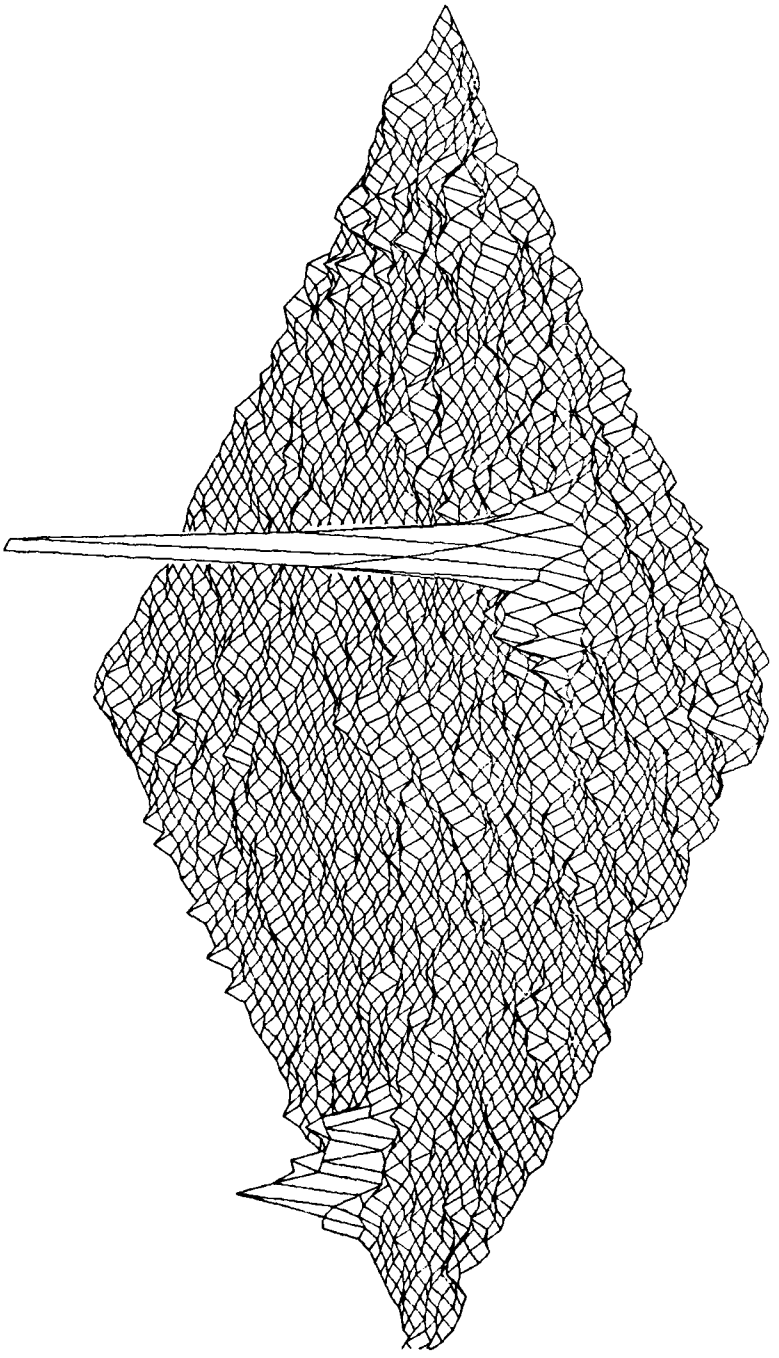

Figure 15. Power distribution of the example scene.

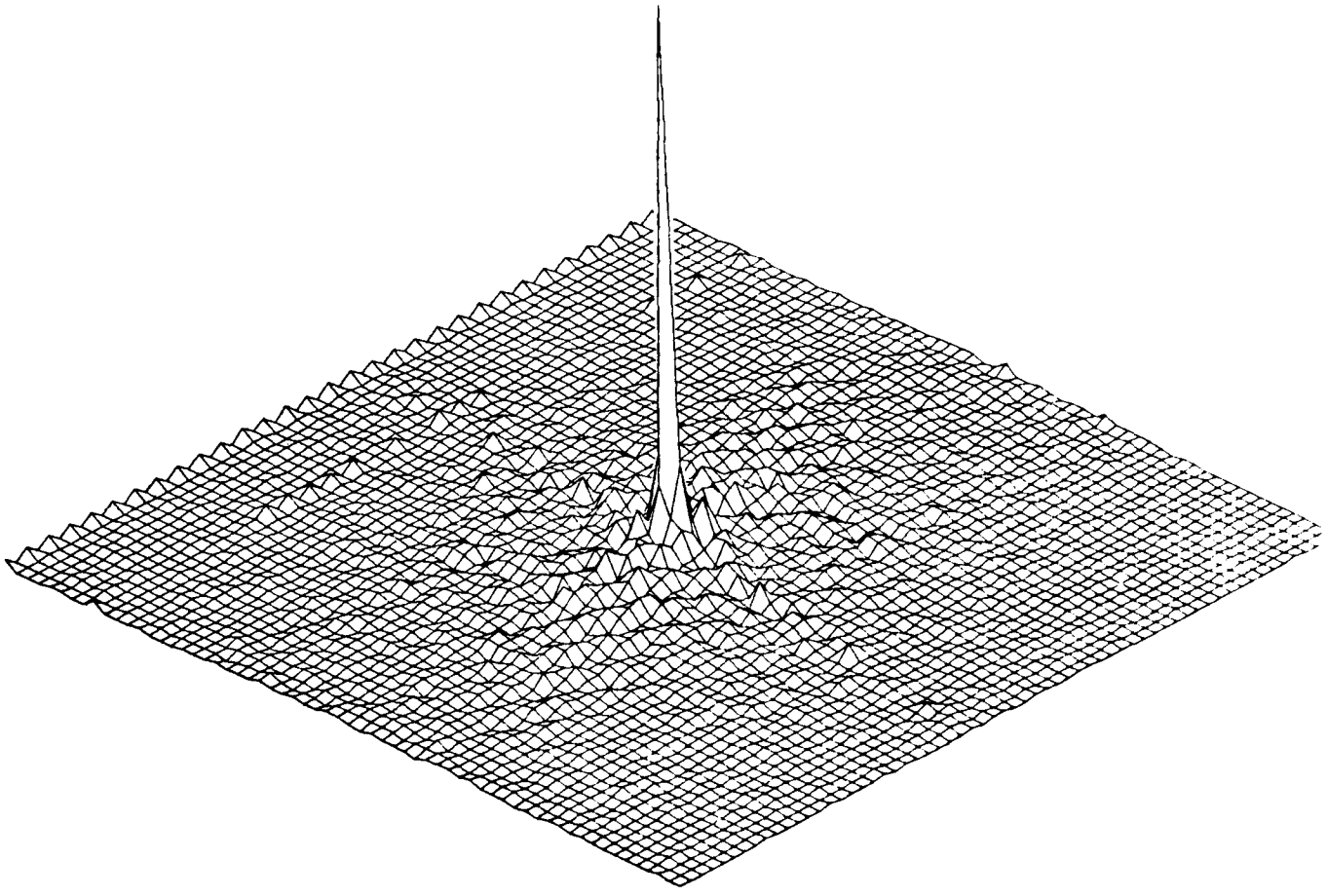

Figure 16. Autocorrelation function in spatial frequency domain.

the scenes would then be inversely transformed and a new set of data calculated to represent Figure 8. The results from this operation should provide more intuitive insight into the problem. This would allow a more sophisticated approach to optimize the frequency bandpass for various clutter conditions.

It is anticipated that, even after maximizing the use of these two variables in complex clutter environments, the loss function will be too large; additional independent samples of data will be required. In anticipation of this, an additional Thermovision in the 8- to 14-μm band has been added to the data collection system. This system will be boresighted with the 3- to 5-μm Thermovision to within one pixel. At the same time this system is added, multispectral data reduction algorithms should be developed.

Appendix A. DATA COLLECTION AND SEEKER SYSTEM MODEL

1. INTRODUCTION

In this section, derivations are given for noise equivalent temperature (NET) for the data collection or seeker system spatial frequency response. Complete and simplified expressions are given; the complete expressions provide a basis for rigorous computer analysis while the simplified expressions provide a means for obtaining reasonable estimates through use of hand calculations.

Neither the concepts nor the final relationships are completely new. The NET derivation is similar to an analysis in Jamieson [1] and Lawson [2]. The frequency dependence and NET expressions are valid for any raster scanned system and may be used for other scan patterns with modifications.

2. TERMINOLOGY

Terminology used in this appendix is consistent with IEEE standard and accepted optical and IR notation. Furthermore, each notation is defined immediately after its use.

3. SEEKER DESCRIPTION

The desired signal information content from a data collection system is the convolution of the spread function of the signal processor with the input signal. When the processor is made up of several components, each spread function must be convolved; however, if the system can be assumed to be linear, then the output signal in frequency space is the multiplication of the transform of the input signal and the transfer functions of the components. Therefore, to determine the type of scene data needed and what data characteristics must be maintained, transfer functions which define degradation of scene information content must be developed.

The breakdown of an IR system as shown in Figure A-1 is considered. The objective optics focus signal energy from the scene which has been degraded by the atmosphere. A mechanical scanner paints the scene onto a detector or detector array or a detector matrix is electronically scanned. The photon sensitive detector transduces the IR energy into an electrical signal which is processed along with the system noise. This processed signal and noise are finally supplied to a set of electronics which, in the case of a seeker system, implement a mathematical tracking algorithm. The quality of these tracking algorithms depends almost entirely on the quality of data in terms of information content and signal-to-noise ratio (SNR). Therefore, if data are to be collected accurately and simulated to these algorithms, the components of Figure A-1 must be defined very accurately. These components can be defined by considering some well-known information theory and IR system

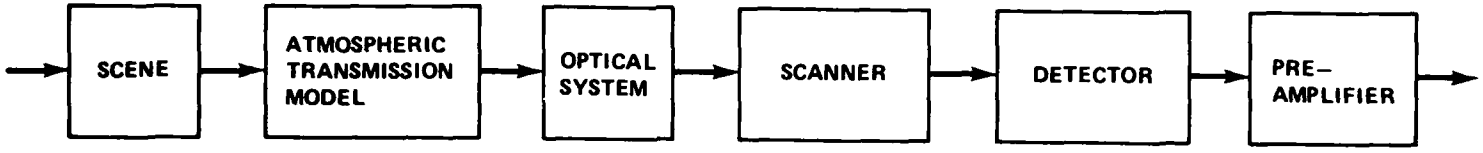

$$(1)\quad v(t) = \int_0^\infty \Delta P(\lambda) * i(t) * r(\lambda, t) * h(t)\, d\lambda$$

$$(2) = \int_{-\infty}^{\infty} e^{-2\pi j f(t)}\, I(f)\, H(f) \left[\frac{r(\lambda, f)}{r(\lambda, f_o)}\right] df \int_0^\infty \Delta P(\lambda)\, r(\lambda, f_o)\, d\lambda$$

Figure A-1. Seeker system model.

merit functions. These theories and merit functions should describe all systems parameters in terms of amplitude and frequency response. In this appendix, NET will be used to define amplitude response, modulation transfer function (MTF) and complex spatial frequency functions used to describe the frequency dependent components. The desired system description can be approached in many ways, but the most efficient and straightforward method appears to be a set of parameters which are divisible into distinct independent entities. If these functions are linear and independent, the net result is achieved by a simple multiplication of the functions.

a. Linear System Considerations

If a data collection system or seeker head is considered as a linear system for all inputs, the output signal will be equal to the input signal convolved with the response function of that system, i.e.,

$$v_o(t) = p_i(t) * h(t) = \int_{-\infty}^{\infty} p_i(t')\, h(t - t')\, dt' \qquad \text{(A-1)}$$

where $v_o(t)$, $p_i(t)$, and $h(t)$ represent the output signal, the input signal, and the system response functions, respectively. The response function $h(t)$ can be defined as the system output function for an input pulse approximating a Dirac delta function. If both sides of Equation (A-1) are Fourier transformed, the expression

$$V_o(f) = P_i(f)H(f) \qquad \text{(A-2)}$$

is obtained. Here $V_o(f)$, $P_i(f)$ and $H(f)$ are the Fourier transforms of $v_o(t)$, $p_i(t)$, and $h(t)$, respectively. The quantity $H(f)$ is referred to as the system transfer function. The one-dimensional (spatial) version of $H(f)$ (i.e., the line spread function Fourier transform) for an optical system corresponds to the system's optical transfer function (OTF) whose absolute value equals the MTF of the system. In Equation (A-2), the quantity $H(f)$ is a filter response which filters the input signal $P_i(t)$. The function $H(f)$ may be divided into many component parts to represent the various system components such as optics, scanner detector, electronics, etc. If these functions act on the signal in a serial manner, the output signal is given by

$$v_o(t) = p_i(t) * h_1(t) * h_2(t) *\ldots* h_{n-1}(t) * h_n(t) \quad ; \qquad \text{(A-3)}$$

correspondingly, the transform of $i_o(t)$ is given by

$$V_o(f) = P_i(f)\ H_1(f)\ H_2(f)\ \ldots\ H_{n-1}(f)\ H_n(f) \quad . \tag{A-4}$$

A wide sense stationary random process (e.g., noise in most electrooptical systems) can be characterized by its autocorrelation function,

$$R(t) = R(t,\ t + \tau) = n(t)\ n(t + \tau) \quad , \tag{A-5}$$

where n(t) designates the random process and τ represents a time difference. The Fourier transform of this function, the power spectrum, is given by

$$S(f) = \int_{-\infty}^{\infty} R(\tau)e^{-2\pi jf(\tau)}\ d\tau \quad . \tag{A-6}$$

The parentheses in Equation (A-5) indicate an average over an ensemble of n(t) functions. The output power spectrum of noise processed (filtered by) a linear system is given by

$$S_o(f) = S_i(f)\ H^2(f) \tag{A-7}$$

where S_o and S_i are the output and input power spectra, respectively. The true relationship between the power spectrum and the variance (at a point) of the random process is

$$\sigma^2 = \int_{-\infty}^{\infty} S(f)df \quad . \tag{A-8}$$

Because negative frequencies are not employed and because S(f) is an even function of frequency, it is common practice to redefine the power spectrum such that

$$\sigma^2 = \int_{-0}^{\infty} S(f)df \quad . \tag{A-9}$$

The power spectrum in Equation (A-9) is twice the one in Equation (A-8). This spectrum is used for temporal voltage noise and the corresponding (horizontal) spatial noise because it is the one most commonly employed by IR systems engineers. In the vertical direction, however, the power spectrum in Equation (8) is used.

A matched filter is a filter whose response function is a delayed (time-shifted) time-reversed (spatially-reversed) version of the signal. Thus, if v(t) is the signal function, the response function of the matched filter is proportional to $v(t_1 - t)$. The matched filter is the filter which maximizes the SNR (signal being the magnitude of the output from the matched filter and noise being the standard deviation of the noise fluctuations) at a time t_1 for the case that the noise is additive (independent of the signal) and white (the power spectrum equals a constant at all frequencies). For the case of a symmetrical signal and for t_1 equal to zero, the matched filter has precisely the same shape as the signal. If

$$V(f) = \int_{-\infty}^{\infty} i(t) e^{-2\pi jf(t)}\, dt \quad , \qquad \text{(A-10)}$$

then the frequency response of the matched filter is proportional to $v^*(f)$, i.e.,

$$H(f) = \int_{-\infty}^{\infty} v(-t)\, e^{-2\pi jf(t)}\, dt = V(f) \quad .$$

b. System Analysis

If an expression for NET is derived in general terms of linear systems analysis, all components of Figure A-1 will then be well-defined. The desired transfer function is of the form

$$\frac{V_o(f)}{I_i(T,f)\sigma} = \tau_a\, G(\Delta T)\, H_o(f)\, H_f(f)\, H_D(f)\, H_E(f)$$

where

$v_o(f)$ = output voltage in terms of spatial frequency

$I_i(T,f)$ = input power in terms of temperature and frequency

$G(\Delta T)$ = system amplitude response

σ = rms noise voltage

τ_a = atmospheric transmission

H_o = optical MTF function

H_f = scanner matched filter

H_D = detector spatial and temporal response

H_E = electronics frequency response.

NET is defined as that input temperature difference for a large target (one whose size is large compared to the system resolution) which is required to generate a signal (voltage amplitude) after the detector preamplifier which is just equal to the rms noise voltage at that point, assuming that the filtering action of the electronics prior to the measurement point corresponds to that of a "matched" filter. Ambiguities in this NET definition provide at least part of the reason NET is viewed with disfavor. However, NET can be a useful indication of system sensitivity and provide a basis for establishing an allowable simulation data noise floor. The only caution here is that when a system is to be simulated, the NET definition and measurement techniques and parameters for that system must be corrected to the "matched" filter definition.

The detector, associated optics, and amplifiers are assumed to be a linear system with a response $r(\lambda, t) * h_c(t)$ where $r(\lambda, t)$ is the detector response in volts/watt and $h_c(t)$ is the system time response function. If the power level incident on the detector equals $\Delta P(\lambda)\ i(t)$ W/μm where i(t) is a normalized time function, the amplifier response is given by

$$V(t) = \int_0^\infty \Delta P(\lambda)\ i(t) * r(\lambda, t) * h_c(t)\ d\lambda \qquad \text{(A-11)}$$

$$= \int_{-\infty}^{\infty} e^{-2\pi j f(t)}\ I(f)\ H_c(f) \int_0^\infty \Delta P(\lambda) r(\lambda, f) d\lambda df \qquad \text{(A-12)}$$

where $I(f)$, $H_c(f)$, and $r(\lambda,f)$ are the Fourier transforms of $i(t)$, $h_c(t)$, and $r(\lambda,t)$, respectively. It is assumed that $r(\lambda,f)$ or $r(\lambda,t)$ are separable into a frequency and wavelength component, i.e., that

$$r(\lambda,f) = [r(\lambda,f_o)] \quad \frac{r(\lambda,f)}{r(\lambda,f_o)} \tag{A-13}$$

where $r(\lambda,f_o)$ is not equal to a function of f, and $r(\lambda,f)/r(\lambda,f_o)$ is not a function of λ. Equation (A-12) is now simplified to

$$V_s = \int_{-\infty}^{\infty} e^{-2\pi jf(t)} I(f)\, H_c(f) \quad \frac{r(\lambda,f)}{r(\lambda,f_o)}\, df \int_o^{\infty} P(\lambda)\, r(\lambda,f_o)\, d\lambda \tag{A-14}$$

$$= i'(t) \int_o^{\infty} P\, r(\lambda,f_o)\, d\lambda$$

where $i'(t)$ is defined in an obvious manner and is addressed in the next session.

1) Amplitude Response

The rms noise voltage corresponding to $V(t)$ must now be determined. Let $S(f)$ equal the detector noise spectrum. The noise power spectrum beyond the preamplifier (i.e., system with transfer function $H_c(f)$ equals $S(f)\, H_c^2(f)$; therefore, the desired rms noise is given by

$$\sigma^2 = \int_o^{\infty} S(f) H_c^2(f)\, df \quad . \tag{A-15}$$

Combining Equations (A-5) and (A-6), the preamplifier SNR is given by

$$SNR = \frac{V(t)}{o} = \frac{i'(t) \int_o^{\infty} P\, r(\lambda, f_o)\, d\lambda}{\int_o^{\infty} \left[S(f)\, H_c^2(f)\, df \right]^{1/2}} \qquad \text{(A-16)}$$

Equation (A-16) yields the NET once the various variables are recast into more useful forms. The SNR is set equal to 1 and i'(t) is set equal to 1. The quantity i'(t) can be set equal to 1 because the signal is determined at approximately the midpoint of an extended target (i.e., low frequency) signal; if i(t) = 1 at its midpoint then i'(t) will also because the signal is of much greater duration than the response function of the detector-amplifier system assumed.

To recast the variables, it is first noted that the detector detectivity, D_λ^* is given by

$$D_\lambda^*(f_o) = \frac{A_d^{1/2}\, r(\lambda, f_o)}{[S(f_o)]^{1/2}} \qquad \text{(A-17)}$$

where A_d equals the detector area. At this point, it is desirable to show similarities with the standard terminology normally used. The more familiar definition of D* is

$$D^* = \frac{(A_d\, \Delta f)^{1/2}}{\Delta P}\, SNR$$

where Δf is bandwidth and SNR is set equal to one. ΔP then by definition becomes NEP and the expression becomes:

$$D^* \quad \frac{(A_d\, \Delta f)^{1/2}}{NEP} \quad .$$

These expressions for D^* are related in the following manner:

$$\text{Detector } SNR_D = \frac{P(\lambda)}{\left[\int_o^{\infty} S(f)\, df \right]^{1/2}}$$

for a small bandwidth around f_o:

$$SNR_D = \frac{\Delta P \; r(f_o)}{[S(f_o) \; \Delta f_o]^{1/2}} \quad .$$

If NEP = ΔP for SNR_D equal to one, then

$$NEP = \frac{[S(f_o) \; \Delta f]^{1/2}}{r(f_o)} \quad ;$$

therefore,

$$D^* = \frac{A_d^{1/2} \; r(f_o)}{[S(f_o)]^{1/2}}$$

Solving Equation (A-17) for (r) and inserting into Equation (A-16), the SNR is given by

$$SNR = \frac{\int_o^\infty \Delta P_\lambda \; D^*(\lambda) \; d\lambda}{A_d \int_o^\infty \frac{S(f)}{S(f_o)} \; H_c^2 df \; ^{1/2}} \qquad \text{(A-18)}$$

where i'(t) has been set equal to 1. Next, it noted that for a simple scanning system,

$$\Delta P_\lambda = \frac{\pi A_d}{4F^2} \; \eta_o(\lambda) \; \frac{\partial L_\lambda}{\partial T} \; \Delta T \qquad \text{(A-19)}$$

where

$\eta_o(\lambda)$ = optical efficiency

F = optical F/number

T = temperature

L_λ = W/cm/sterad/μm.

Finally, using Equation (A-19) for ΔP_λ and defining Tf by:

$$\Delta f = \int_0^\infty \frac{S(f)}{S(f_o)} \; H_c^{\,2} \; df \quad , \tag{A-20}$$

Equation (A-18) becomes

$$SNR = \frac{\pi A_d^{1/2} \Delta T \int_0^\infty \eta_o(\lambda) \frac{\partial L}{\partial T}_\lambda D^*_{f_o}(\lambda) \, d\lambda}{4F^2 (\Delta f)^{1/2}} \quad . \tag{A-21}$$

The ΔT in Equation (A-21) is the desired NET provided the SNR is set equal to 1 and provided the bandwidth equals the approximate reference bandwidth.

The bandwidth to which NET is commonly referenced is given by:

$$\Delta f = \frac{\pi}{2} f_o = \frac{\pi}{2} \left[\frac{(XFOV)\ (YFOV)\ F_R\ \eta_{os}}{2\ n_p\ X\ Y\ \eta_{se}} \right] \quad . \tag{A-22}$$

where

XFOV = horizontal FOV (mrad)

YFOV = vertical FOV (mrad)

F_R = frame rate, for interlaced systems F_R = field rate

η_{os} = overscan ratio

n_p = number of lines scanned in parallel

X = horizontal instantaneous FOV (IFOV)

Y = vertical instantaneous FOV

η_{se} = scan efficiency (ratio of active scan to total scan).

The initial form of Δf in Equation (A-22) is obtained from Equation (A-20) first by setting the power spectrum ratio equal to 1 (i.e., ignoring all low frequency 1/f components and high frequency roll-off)

and secondly by equating H_c^2 to

$$\frac{1}{[1 + (f/f_o)^2]}$$

corresponding to an exponential response function for the electronic circuitry. The expression for f_o is derived by setting f_o equal to $1/2\tau_d$ where τ_d is the delay time for a resolution element of size X, Y (essentially the time the detector element spends on each resolution element). The $1/2\tau_d$ corresponds to

$$\int_o^{\infty} \left[\frac{\sin(\pi f \tau_d)}{\pi f \tau_d}\right]^2 df$$

which is the bandwidth associated with a rectangular function of duration τ_d.

Some additional expressions and definitions are useful in defining a given seeker system. First D* is given by

$$D^*_\lambda = \frac{D^{**}_\lambda}{\sin\Phi/2} = \eta_{cs} D^{**}_\lambda \qquad \text{(A-23)}$$

where

$D_\lambda^{**} = D_\lambda^{*}$ for no cold shield

η_{cs} = cold shield efficiency

Φ = cold shield angle.

The quantity W is defined by

$$W = \int_o^{\infty} \frac{\eta_o(\lambda)\ D^*_{fo}(\lambda)}{\eta_o(\lambda_p)\ D^*_{fo}(\lambda_p)} \frac{\partial L}{\partial T} d\lambda \qquad \text{(A-24)}$$

where λ_p = wavelength for peak $D^*_{fo}(\lambda)$.

For most seekers, Equation (A-23) does not apply because cold shields are not normally employed.

The NET, using Equation (A-24) is given by

$$NET = \frac{4F^2(\Delta f)^{1/2}}{\pi A_d^{1/2}\ \eta_o(\lambda_p)\ D^*_{fo}(\lambda_p)W} \qquad (A\text{-}25)$$

where Equations (A-22), (A-23), and (A-24) provide useful expressions for f, $D^*_{fo}(\lambda)$, and W. A_d may be converted to optical element units by the relationship

$$A_d = (\text{focal length})^2\ (\text{IFOV}) \quad .$$

2) Spatial Frequency Response

The signal frequency dependence can be determined by referring to Equation (A-11). Equation (A-12) was divided into a frequency and wavelength dependent component in order to solve for NE t and SNR as a function of input data wavelength and T. If Equation (A-12) is recast into the form

$$\frac{V(t)}{\sigma} = \int_{\infty}^{\infty} e^{-2\pi jf(t)}\ I(T,f)\ H_c(f)\ G(\ T)df \qquad (A\text{-}26)$$

the frequency dependence can be treated. G(T) is represented by Equation (A-21) and is not a function of frequency but represents the seeker amplitude response. It must be remembered that the conditions of Equation (A-21) were that the noise power spectrum is limited to f_o and that D^*_λ is not a function of frequency. This does not severely restrict its usefulness because the modifications are very simple.

If Equation (A-26) is transformed to

$$\frac{v(f)}{\sigma} = G(\Delta T)\ I(T,f)\ H_c(f) \qquad (A\text{-}27)$$

where

$I(T,f)$ = input as a function of temperature and frequency

$H_c(f)$ = seeker head filter function

$G(\Delta T)$ = seeker response as a function of temperature.

The only remaining chores are to determine the form of $H_c(f)$ for the various components where

$$H_c(f) = H_o(f)\ H_f(f)\ H_D(f)\ H_E(f) \qquad \text{(A-28)}$$

where

$H_o(f)$ = optical MTF functions

$H_f(f)$ = scanner and matched filter MTF

$H_D(f)$ = detector MTF

$H_E(f)$ = lectronics MTF.

a) Optical MTF Functions

There are many options in the calculation of optical MTF functions, but in general, the MTF function is the product of a diffraction limited component and a Gaussian abberration (or blur) component. The diffraction limit MTF as a function of spatial frequency f_x (cycles/mrad) for optics with F number ($F^{\#}$), and at wavelength λ is given by

$$H_{od}(f) = \frac{2}{\pi}\left\{\cos^{-1}(c_1 f_x) - c_1 f_x \left[1 - (c_1 f_x)^2\right]^{1/2}\right\} \qquad \text{(A-29)}$$

where $c_1 = \lambda F^{\#}$.

If cylindrical symmetry is assumed, Equation (A-29) is valid for the vertical transfer characteristic also. The Gaussian geometric blur can be considered as

$$H_{og}(f) = e^{-c_2 f_x^2} \qquad \text{(A-30)}$$

where C_2 is evaluated (or measured) at a specific data point and is

given in terms of (K) at K_1 cycles/mrad where K will always be less than one because the data point is on the exponential part of the frequency curve. The total MTF function can then be calculated as

$$H_o(f) = \frac{2}{\pi}\left\{\cos^{-1}(c_1 f_x) - c_1 f_x\left[1-(c_1 f_x)^2\right]^{1/2}\right\} e^{-c_2 f_x^2} \quad . \quad \text{(A-31)}$$

b) Matched Filter

The scanner filter transfer function is identical to the NE T "standard" noise filter bandwidth. This function also represents the signal maximum bandwidth assuming that all other MTF functions are one over the frequencies of interest:

$$f = f_o/2$$

$$= \frac{}{2}\left[\frac{(HFOV)(VFOV)\ F_R\ \eta_{os}}{2\ n_p\ x\ y\ \eta_{sc}}\right] \quad . \quad \text{(A-32)}$$

In this case, the frequency is an electrical frequency and must be converted back to spatial coordinates by the following linear transformation:

$$f_x = \frac{f(H_z)}{V_s(\text{mrad/sec})} \quad \text{(A-33)}$$

where V_s is the detector scan velocity in milliradians per second. The scanner matched filter transfer function then becomes

$$H_f(f) = \frac{1}{1 + jf_x/f_{xo}} \quad . \quad \text{(A-34)}$$

Combining Equations (A-32), (A-33), and (A-34), the frequency dependent components due to the scanner and matched filter are obtained:

$$H_f(f) = \frac{1}{1 + j\ f_x V_s \Big/ \left[\dfrac{(HFOV)(VFOV)F_R\eta_{os}}{2\eta_p\ x\ y n_{se}}\right]} \quad \text{(A-35)}$$

c) Detector Spatial and Temporal Response

The detector response is normally divided into a spatial component and a temporal component. However, for most seeker systems the temporal response is negligible. The temporal response will be covered only for completeness.

Spatial filtering in the horizontal or vertical direction is given by

$$H_D(f) = \frac{\sin(\pi f_x \Delta x)}{\pi f_x \Delta x} \qquad \text{(A-36)}$$

where Δx is twice the detector scan direction, IFOV.

The detector temporal response is significant only when the detector dwell time is very short. When this occurs, charge carriers in the detector material do not respond fully to scene changes at higher spatial frequencies. This phenomenon can be represented by a simple first order lag of the form

$$H_{D_T}(f) = \frac{1}{1 + jf_x/f_x^*} \qquad \text{(A-37)}$$

where f* is the conventional detector 3-dB break frequency (Hz) converted to spatial frequency in cycles/milliradian by the relationship of Equation (A-33).

d) Electronics

Electronics beyond the already assumed matched filter associated with the scanner system can only filter the signal temporal characteristics. Filtering beyond the matched filter can be modeled by cascading either first order leads or lags. The first order leads are modeled as

$$H_E(f) = 1 + jf_x/f_{ox} \qquad \text{(A-38)}$$

where f_{ox} and f_x are converted to spatial frequency by the constant scan velocity. Lag networks are identical to Equation (A-37) after conversion to spatial frequencies. If the input signal mean value (or dc term) is important, all seeker lead terms must be modelled as in Equation (A-38).

3) Seeker Transfer Function

Combining the previous results, the desired seeker transfer function is obtained:

$$\frac{V_o(f)}{I_i(T_j f)} = \tau_a \, G(\,T)\, H_o(f)\, H_f(f)\, H_D(f)\, H_E(f) \qquad \text{(A-38)}$$

where τ_a is the atmospheric transmission, $H_o(f)$ is the optical transfer function given by Equation (A-31), $H_f(f)$ is the scanner and matched filter transfer function given by Equation (A-35), H_D is the detector transfer function given by Equations (A-36) and (A-37), $H_E(f)$ is the electrical transfer function as described in Equations (A-37) and (A-38), and $G(\,T)$ is the amplitude response given by Equation (A-21). These results are shown in Figure A-2.

4. DATA FORMAT

Equation (A-39) defines either the seeker or data collection system; to determine the required data format, each component must be investigated. If a simple filter function is considered, the frequency dependence can be readily explained and the effects of each term of Equation (A-39) become obvious. The simple function

$$\frac{P_o(f)}{P_i(f)} = \frac{K}{1 + jf_x v/f_o} \qquad \text{(A-40)}$$

is considered where $P_o(f)$ and $P_i(f)$ are the output and input power, f_o is the filter break frequency and v is the scan velocity in milliradians/second. The only point which must be remembered is that each filter function will have an effect directly proportional to its break frequency. Only the magnitude term is of concern here. The filter functions may be represented as complex functions to maintain phase, but it is not necessary to explain the frequency versus magnitude signal characteristics. The magnitude as a function of spatial frequency is as shown in Figure 15 with the frequency break point at V/f_o. This break frequency is in terms of cycles/milliradian and is independent of range.

If Figure A-3 is now converted to a function of range (R), the frequency variable is converted from cycles/milliradian to cycles/meter ground resolution where R is defined in meters. Equation (A-40) then becomes

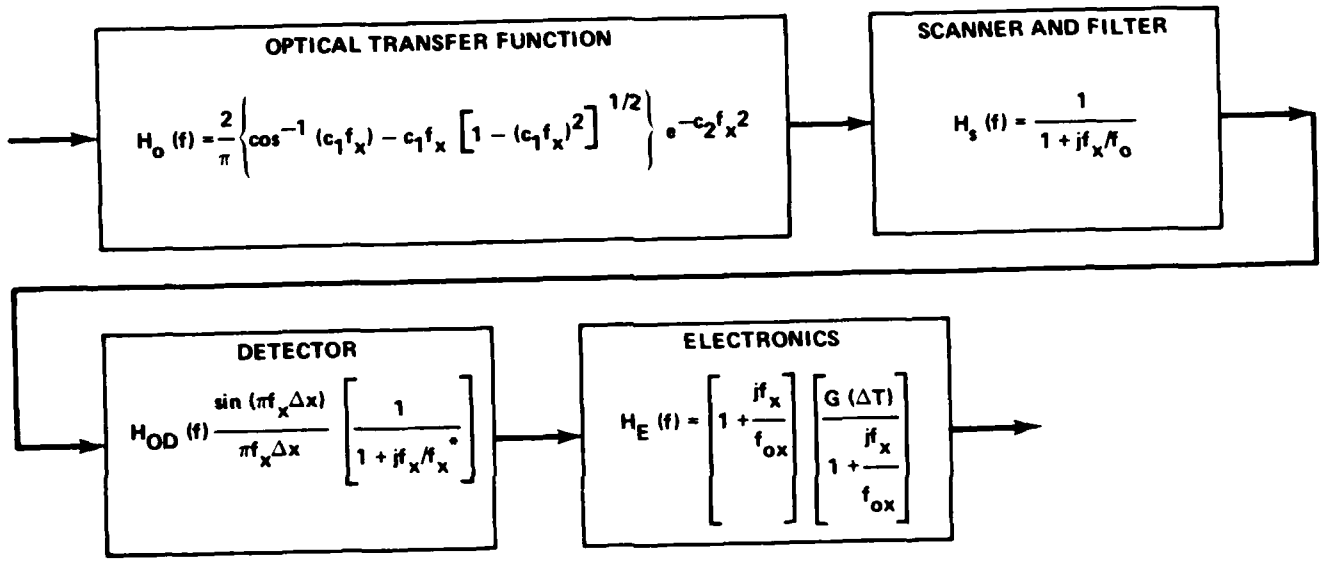

$$f\,(\text{Hz}) = \frac{\pi}{2}\left[\frac{(\text{HFOV})\,(\text{VFOV})\,F_{R\eta os}}{\eta_p \Delta x \Delta y \eta_{sc}}\right]$$

$$f_x\,(\text{CYCLES/mrad}) = f\,(\text{Hz})/V\,(\text{mrad/sec})$$

$$f_x\,(\text{CYCLES/m}) = f_x\,(\text{CYCLES/mrad})/R\,(\text{m})$$

Figure A-2. Seeker transfer functions.

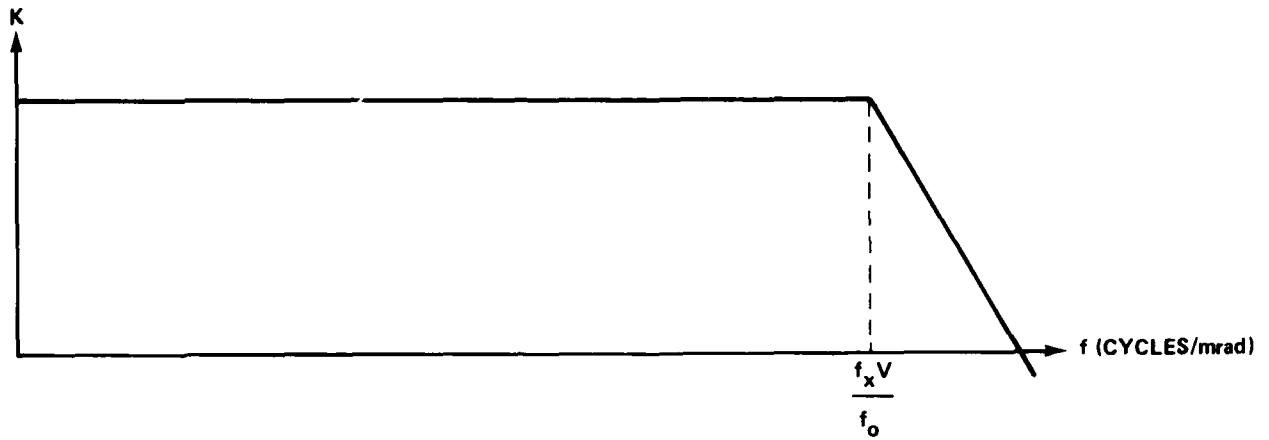

Figure A-3. Matched filter magnitude frequency (cycles/mrad).

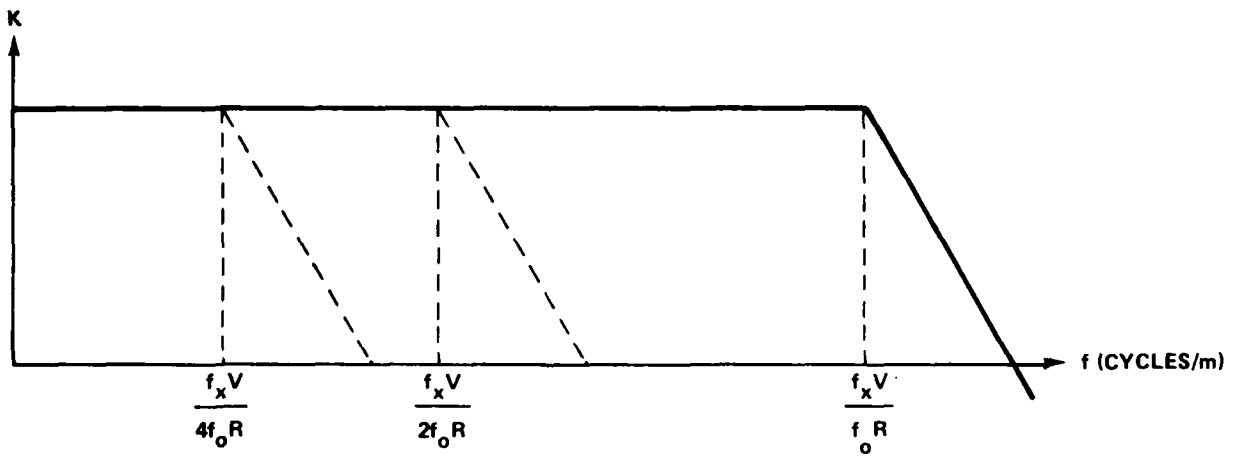

Figure A-4. Matched filter magnitude frequency (cycles/m) plot.

$$\frac{P_o(f)}{P_i(f)} = \frac{K}{1 + jf_x\, v/Rf_o} \quad . \qquad \text{(A-41)}$$

Again, this is a linear transformation and does not violate the assumptions of linear systems or mathematical principles. All frequency dependent terms of the seeker transfer functions may be converted by the factor

$$f(\text{cycles/m}) = f(\text{cycles/mrad}) \quad 1/R \ (\text{m}) \qquad \text{(A-42)}$$

If Equation (A-41) is now represented by a magnitude versus frequency plot (Figure A-4), a family of curves is obtained (one for every value of R). In this representation, the required data format ground resolution can be determined as a function of range. As range decreases by a factor of two, the seeker resolution (cycles/meter) also increases by a factor of two. This will ultimately limit the minimum range simulated from a given data set. For example, if the desired range closure simulation is from 4096 m down to 128 m the seeker resolution in meters increases by a factor of 32. (Figure A-5).

Equation (41) shows the highest resolution to be at minimum range and decreases inversely proportional to range. This implies that, if real world data are collected and used while maintaining the true information content, the following scale factor between the seeker and data collection system must be maintained as well as matching the FOV (Figure A-6).

$$\frac{f_{xs} V_s}{R_s f_{os}} \leq \frac{f_{xd} V_d}{R_d f_{od}} \quad . \qquad \text{(A-43)}$$

Here s and d represent the seeker and data collection device, respectively. If the conditions of Equation (A-43) cannot be met, then the seeker and data collection system must be matched at some value of range (r). The data set is then degraded in a controlled fashion to match the seeker system response. In the case where the conditions of Equation (A-43) cannot be met, the data would not be degraded using the seeker transfer functions, but would use an artificial set of functions. The result would be identical to a high resolution data set degraded by the seeker transfer functions.

Appendix A shows a simple method of data degradation utilized by Night Vision Labs (NVL) in the TLGP simulation. This approach is valid only when the seeker system under consideration has infinitely small resolution capability. For example, all of the components of Equation (A-39) for the data collection system are assumed to have spatial

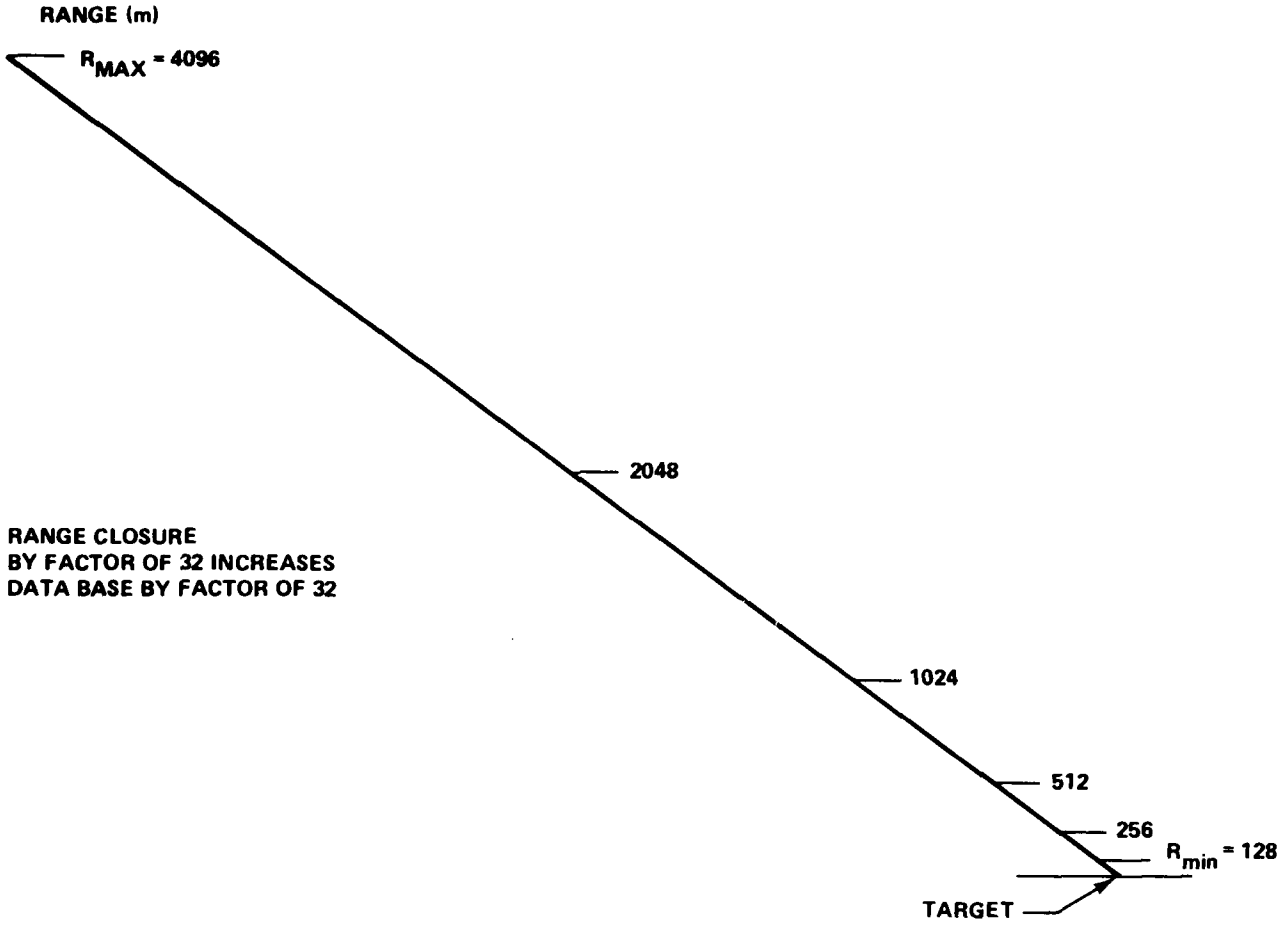

Figure A-5. Range scaling.

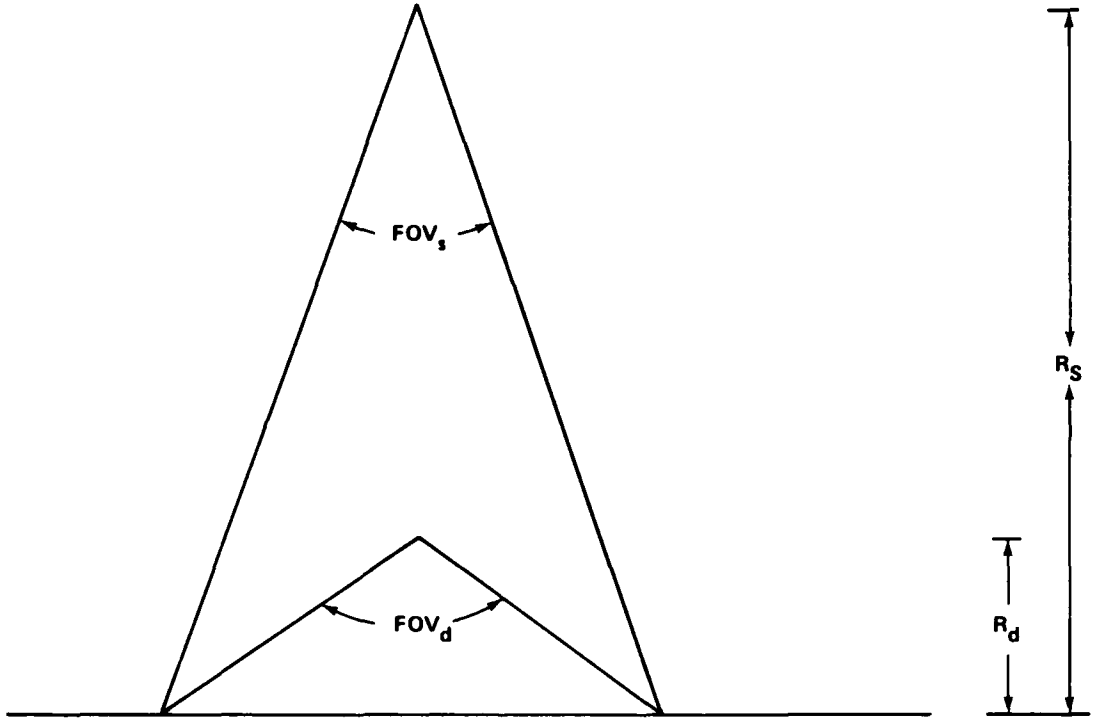

$R_S \tan FOV_s = R_d \tan FOV_d$ AT MAXIMUM R_s

R_S = SEEKER RANGE

R_d = DATA COLLECTION SYSTEM RANGE

Figure A-6. FOV matching.

frequency responses well above the seeker. Now if the data are degraded simply by matching the IFOV, all high frequency data components are maintained. These high frequency components are supplied directly to the seeker processor and do not represent a valid simulation. For example, a simple case is considered where it is desired to simulate range closure by a factor of three with a data set taken at the shortest range. The IFOV is matched by the following method:

$$R_s \tan \text{IFOV}_s = R_d \tan \text{IFOV}_d \quad . \tag{A-44}$$

For this condition, the data at the longer range R contain more high frequency data than the seeker would normally see. This is easily shown by considering the one-dimensional case where the scene data contain a square wave with a period equal to two resolution elements (Figure A-7). These data can be represented by the sums of Fourier series components representing the square wave as:

$$\frac{4K}{} (\sin f_x + 1/3 \sin 3f_x + 1/5 \sin 5f_x + \ldots) \quad . \tag{A-45}$$

It can be seen that if the data are degraded by simply taking the data mean value of two resolution elements, all high frequency components are maintained. However, when the true optical MTF function is used as a spatial frequency filter as

$$H_o(f_x) = \frac{1}{\left[1 + (f_x/f_o)^2\right]^{1/2}} \quad , \tag{A-46}$$

frequencies near or above the optical cutoff, f_o, will be attenuated identically to those of the seeker.

The first case, where data are degraded simply by taking the mean value of several resolution elements, enhances all edge information. However, the true filter in Equation (A-46) attenuates the higher frequency components. In fact, the high frequency third harmonic energy never reaches the focal plane. This can also be shown by data reduction techniques. Figures A-8 through A-12 show a 900 × 900 resolution element scene, a power plot of the scene filtered to 128 by 128 resolution elements, the Fourier Transform magnitude plot (autocorrelation function), and the inverse transform power plots after the scene has been filtered by a single simple optical MTF function to represent a 25% and 50% range difference in observing the data. Figure A-13 shows a 64 × 64 resolution element power plot which has been reduced by 0.50% in range using the y mean value method.

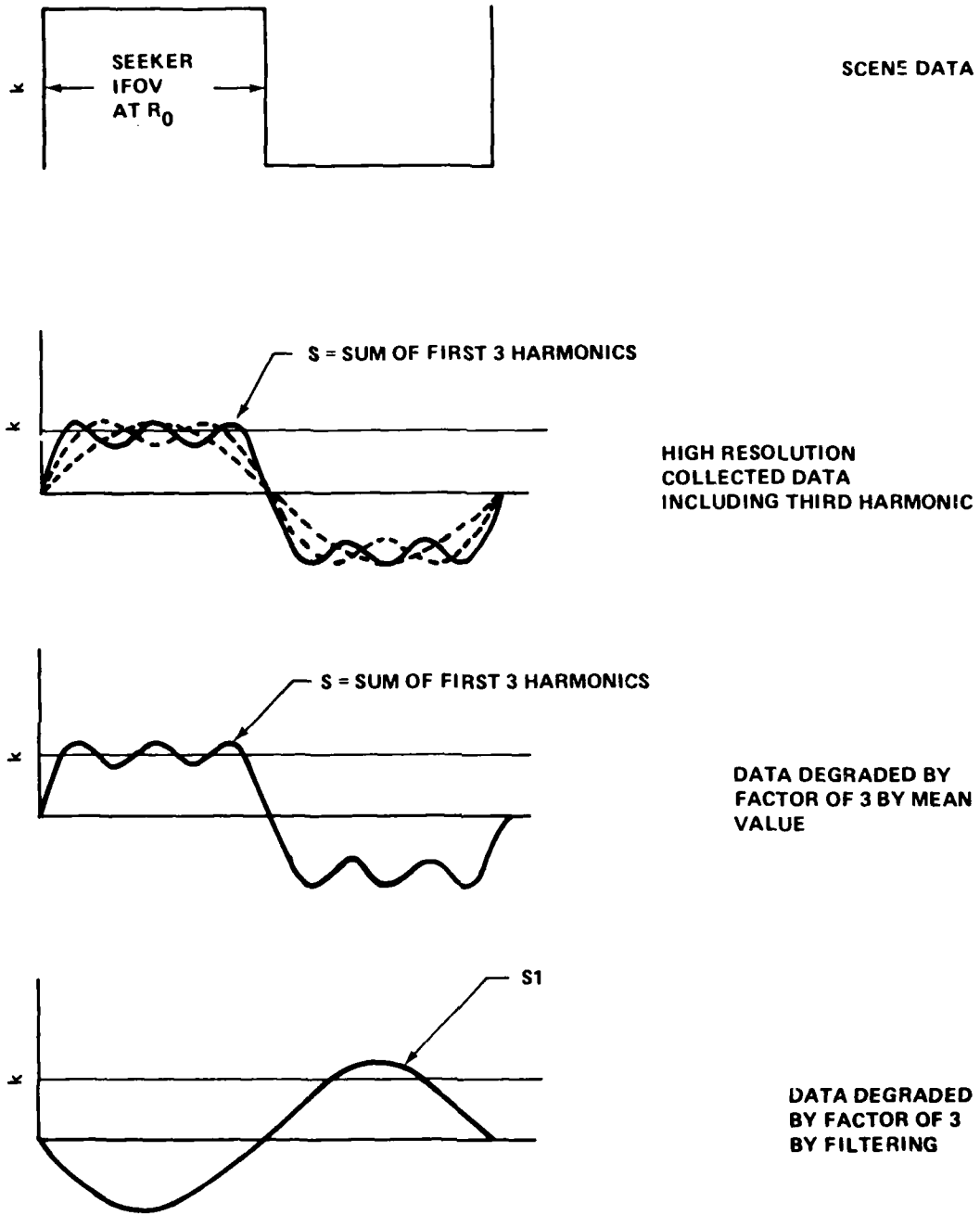

Figure A-7. One-dimensional data format.

Figure A-8. Scene 1 900 × 900 resolution element power plot (8 to 14 μm).

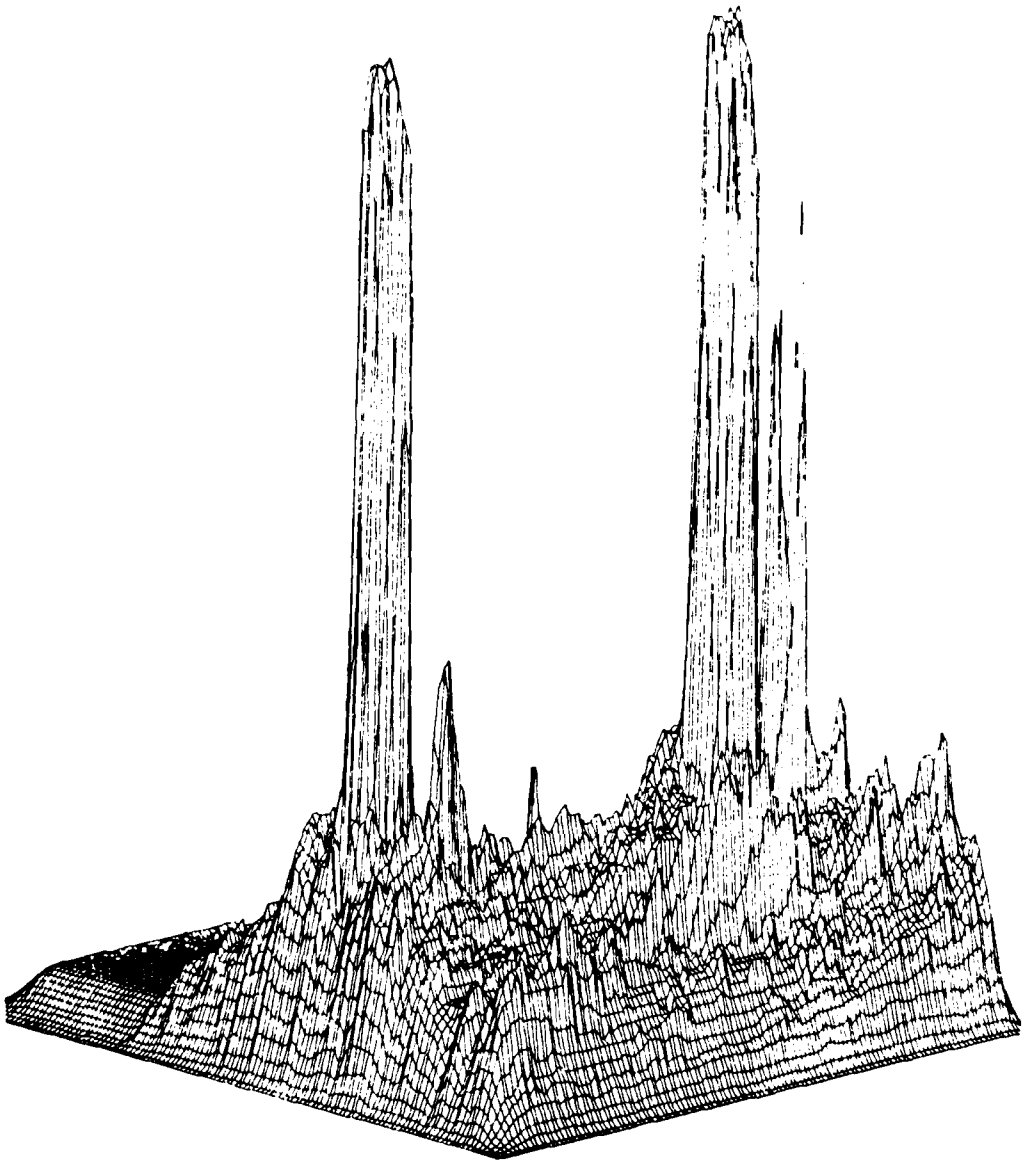

Figure A-9. Scene 1 128 × 128 resolution element power plot.

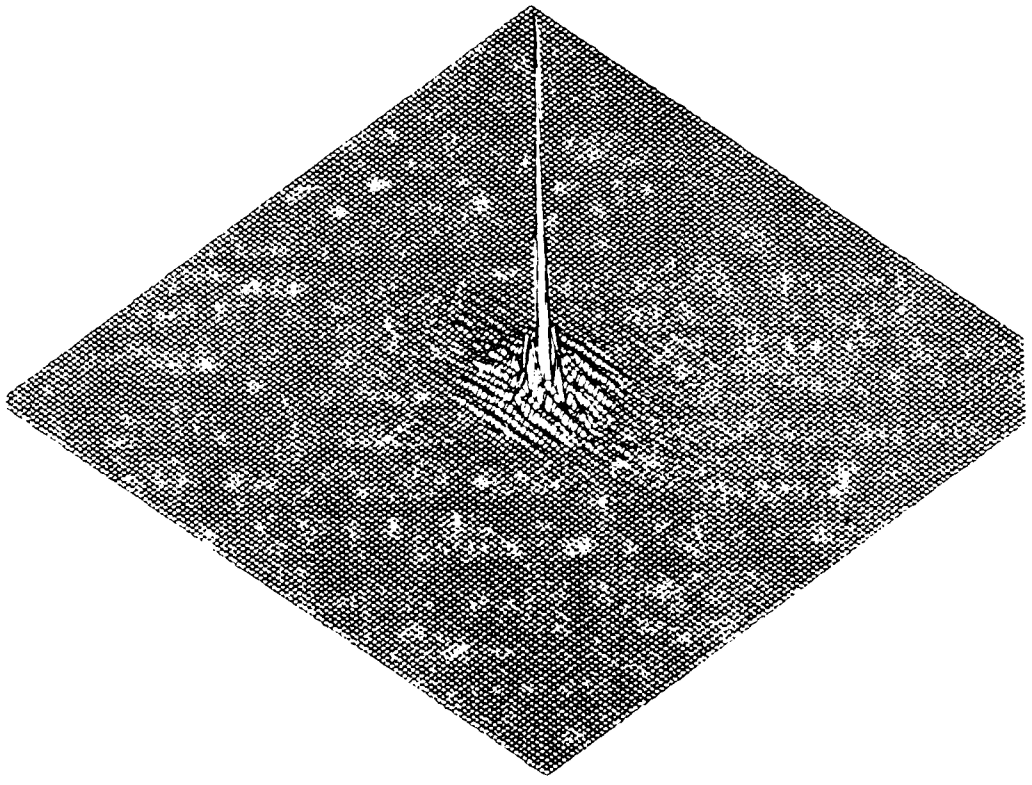

Figure A-10. Scene 1 Fourier transform of 128 × 128 resolution element data.

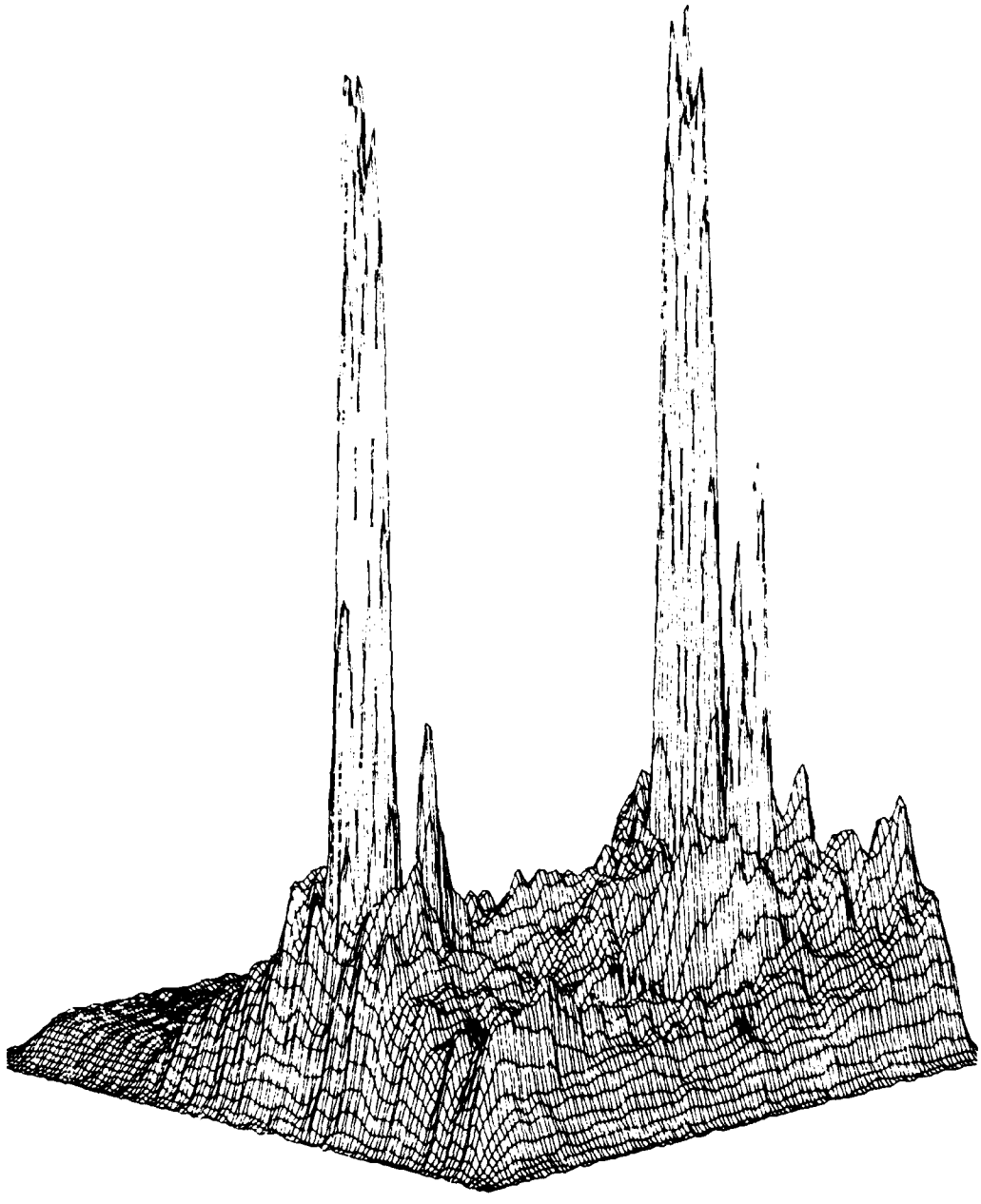

Figure A-11. Scene 1 frequency filtered to 96 × 96 resolution elements, single order lag.

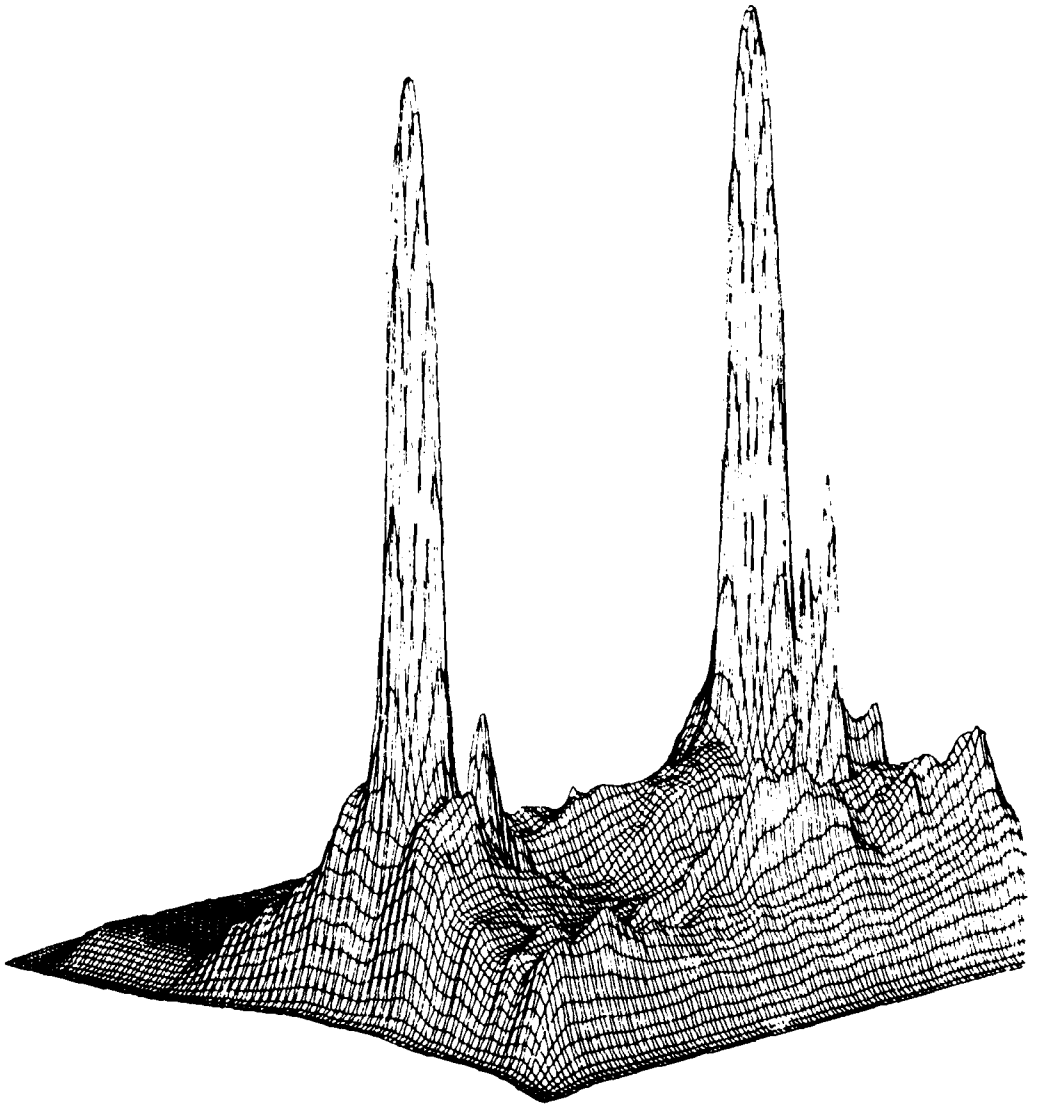

Figure A-12. Scene 1 frequency filtered to 64 × 64 resolution elements, single order lag.

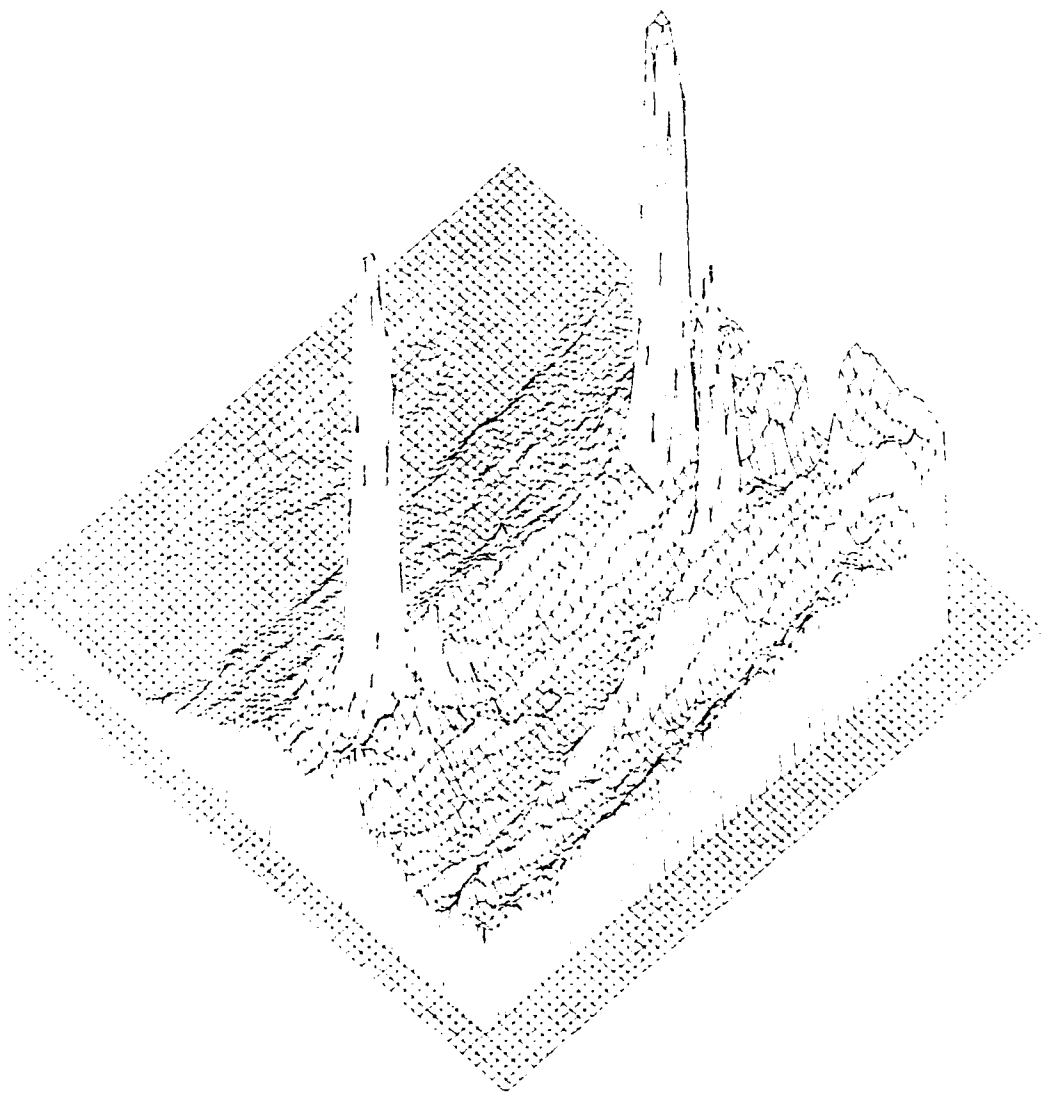

Figure A-13. Scene 1 resolution reduced to 64 × 64 resolution elements, mean value method.

The 64 × 64 resolution element power plot in Figure A-12 was obtained by applying a circular filter in the Fourier transformed scene frequency domain. The circular filter simply implies that the data resolution was reduced equally in all directions in the frequency domain. In object space, this has the effect of degrading vertical, horizontal, and diagonal edges equally. This filter function is equivalent to an optical MTF for a circular aperture system. In Figure A-9, a window function has been applied to the scene to eliminate high frequencies created by the artificial step function at the physical data limits. All comparisions should be made on internal scene detail without consideration of the scene data edges. After comparing Figures A-12 and A-13, it becomes obvious that the filter function is preferred over the mean value method. However, the mean value is a close approximation except for the case where an algorithm has differentiation.

Previous results show effects of an optical system Gaussian aberration MTF functions. All other filter functions will have a similar effect and should be treated similarly. The one exception is a raster format line scanning detector spatial function. As seen earlier, the detector spatial frequency function is represented by

$$H_D(f) = \frac{\sin \pi f_x \Delta x}{\pi f_x \Delta x} \qquad \text{(A-47)}$$

where Δx = 2 IFOV.

Observing the minima and maxima of this function, zeroes occur at frequencies where f_x is the reciprocal or the even multiple of the reciprocal of Δx. Maxima occur where f_x is half multiples of the reciprocal of Δx. The primary question then is what information content the signal contains. A good discussion of this subject may be reviewed from References 1 and 2. These references show that 91% of the total energy is contained within the spectrum between zero and the first null of $H_D(f)$ corresponding to a frequency equal to the reciprocal of Δx. The y direction filtering function is identical to the x direction for a square detector. These facts imply that the maximum frequency content of the rectangular function is a frequency whose period is the reciprocal of two resolution elements. This remains true for all cases except where high energy point sources of less than one resolution element spatial extent are present in the scene.

The last filter function to be considered is the sampling process created by sampling the collected data. If this process is considered as independent of other filter functions, then the scanning optical system unambiguously samples object space at sample intervals equal to

the IFOV. The sampled data theorem is normally referred to a time domain but presents no problems to a spatial frequency reference in cycles/meter.

If data are considered as periodic, the lower bound sampling rate is

$$N \geq 2K + 1 \tag{A-48}$$

where N is the number of samples per fundamental period and K is the highest harmonic in the Fourier series for f(x). If N is the number of samples per fundamental period and if a period consists of x m, then the sampling rate must be N/x samples/m and the highest frequency component in the Fourier series representation of f(x) must be K/x cycles/m. K, x, and N must now be related to the seeker or data collection system to the total FOV, IFOV, and Range. If N is the number of resolution elements per scan line:

$$N = \frac{FOV}{IFOV} \quad . \tag{A-49}$$

Substituting this value of N into Equation (A-48), K is obtained as

$$K \simeq \frac{FOV}{2IFOV} \quad . \tag{A-50}$$

The spatial frequency resolution is then given by

$$\frac{K}{x} = \frac{1}{2R(IFOV)} \quad \frac{cycles}{m} \tag{A-51}$$

where x is the ground coverage in meters and given by (R)(FOV). The highest scene harmonic is given by Equation (A-50) while the highest spatial frequency resolution is given by Equation (A-51). Unlike the other filter functions which have complex frequency responses and roll off the higher order frequency components in an exponential fashion, the sampling process creates an infinite attenuation to all frequencies above cutoff.

5. SUMMARY AND CONCLUSIONS

Seeker system simulations with real tactical data are at best a difficult and tedious task. Figure A-2 represents a set of transfer functions which are valid for the data collection system and the seekr system to be simulated. These transfer functions must be evaluated for both systems. Initially, the data collection system must be evaluated to determine the collected data quality. Figure A-14 shows the asymptotes of magnitude versus frequency for each transfer function and the

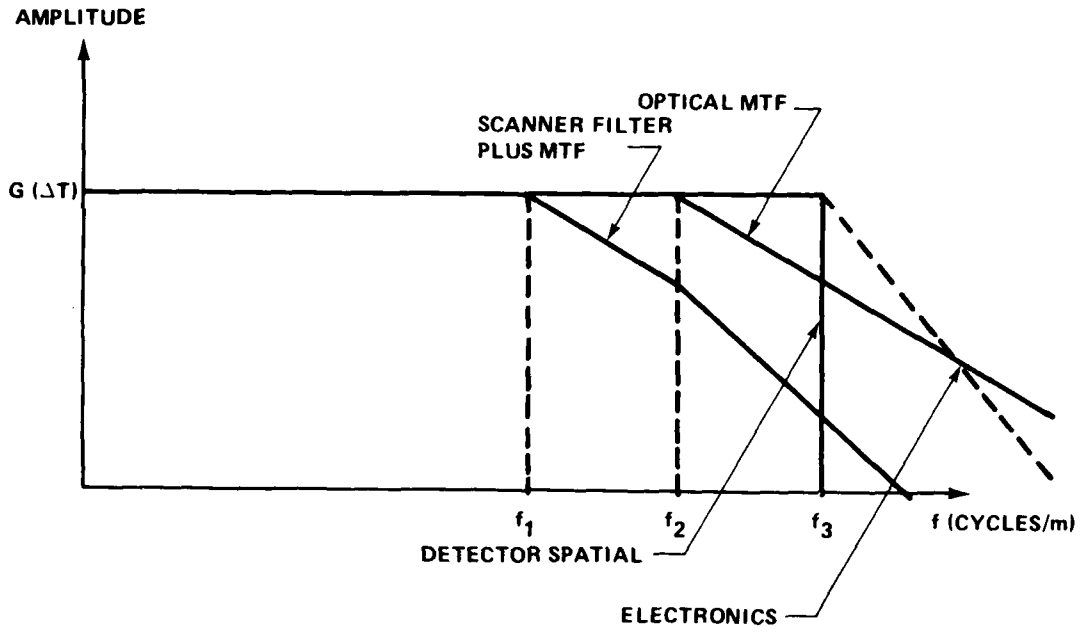

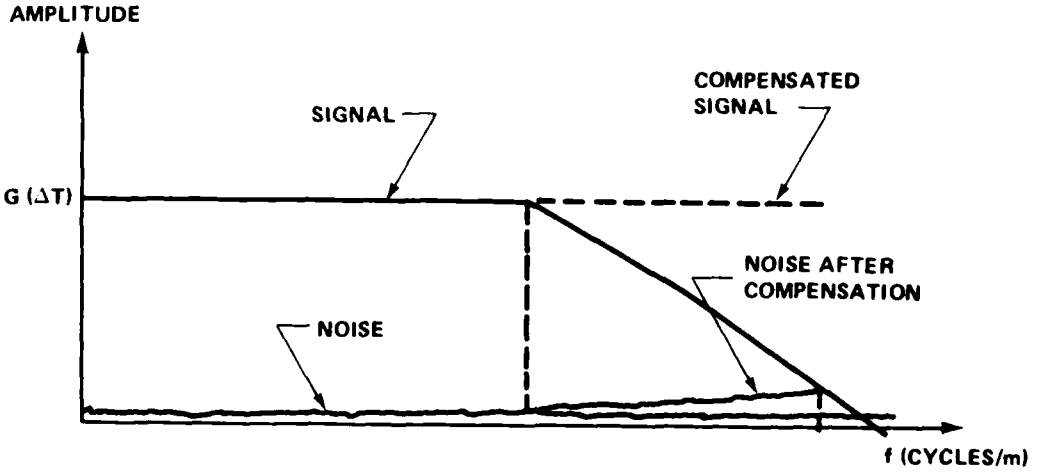

Figure A-14. Seeker frequency response.

accumulative response. Obviously, valid data exist only out to a resolution frequency f_1 and represent the minimum seeker resolution which can be simulated by these data. Data frequency response corrections may be made by multiplication of the data by an inverse function of the accumulative response. These correction limits are established by the NE T noise floor and where it intercepts the signal response function. Correction beyond a frequency where $f_x = f_c$ on the accumulative response function will degrade SNR of the original data collected. This new value of noise also establishes a new noise floor and changes the data SNR. It must also be remembered that, in general, the noise will be affected only by the detector temporal response and electronics. After this complete definition of data quality and correction procedures, the data can be digitized at twice the corrected frequency f_c. Alternately, the data could be collected, digitized at twice f_c, Fourier transformed, and then the appropriate frequency components corrected. This data set could be used with full confidence and without rationalization.

Independent of how the seeker simulation is implemented, the transfer functions of Figure A-2 must be evaluated for that system. After the initial evaluation, it may become obvious that some functions are negligible; however, to match the seeker resolution to a data set, the evaluation must be made. Matching the seeker resolution to a data set at a range, R, determines the minimum range which may be simulated with that data.

The FOV matching problems make it impractical to take data at the minimum range. For example, if the data collection system and seeker have identical spatial frequency responses, the data system FOV must be a factor of 32 larger to simulate range closure from 4096 to 128 m. To solve this problem, data must be taken at several points along the line-of-sight to the target. Alternately data could be taken by a zoom optical system.

The primary considerations here have been to consider an all-digital simulation for seeker systems which collect data in a raster format but the techniques are not necessarily limited to these systems. Any system whose optical system and scanner can be defined in a closed mathematical form may be simulated by these techniques. If a scanner is nonlinear and can be quantized into a reasonable number of linear increments, the method is still valid. These methods are also practical when it is desired to segment a scene and evaluate a seeker acquisition problem.

The sequence which should be followed to do this simulation is as follows:

a) Evaluate data collection system.

b) Evaluate seeker transfer functions.

c) Determine correct range for data collection.

d) Collect and digitize data at the seeker operational wavelength (Appendix B).

e) Edit data using graphics terminal or plotter outputs.

f) Perform data analysis as follows:

   1) Three-dimensional power plots at each point in the quasi-static simulation.

   2) Scene histogram.

   3) Statistical analysis, scene mean and deviation, target mean and deviation.

g) Fourier transform data (two-dimensional).

h) Implement seeker filter functions.

i) Complete simulation.

6. RECOMMENDATIONS

Because the primary purpose of simulations is to evaluate seekers, it is desirable to understand why a system does or does not function properly. To make these interpretations, it is necessary to display to the observer both the data being used by the seeker system and the data which have been filtered from the scene. To accomplish this, it is necessary to use a display which has the capability of storing one entire scene and taking the difference between the original data and the filtered data. Therefore, if this type display is not available, it is strongly recommended that one be purchased.

Appendix B. CLASSIFIER MODEL FOR DISCRIMINANT SYSTEMS

1. INTRODUCTION

Everyone is an expert at target-background discrimination but virtually nothing is known about it. Perception of the environment (target/background discrimination) is performed constantly by all living creatures but little is known about the actual processes involved because most occur at the subconscious level. The idea behind research in pattern recognition is to model the processes of perception to enable computer systems to perform interpretation (rather than manipulation) of sensed data.

2. MODEL OUTLINE

The classifier model is an approach which uses a flexible combination of heuristic and statistical means to select and/or evaluate an optimal target/background discrimination system. Extensive reviews and detailed descriptions of the classifier model and other pattern recognition systems are available in the literature [1 - 8]. The authors will here recap a general outline of the model using examples and illustrations to allow the reader to become familiar with the working concepts of pattern recognition as applied to target/background discrimination. The classifier model consists generally of three different parts (Figure B-1).

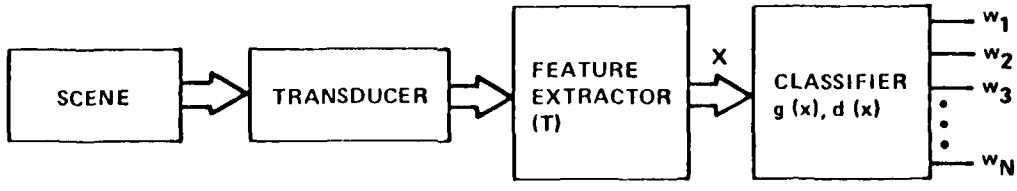

Figure B-1. The classifier model.

a. Transducer

The transducer essentially defines the observation set. That is, the transducer senses or measures the external environment and converts that information into a machine-usable form. In mathematical terms, the transducer generates p-dimensional observation vector, $y = \{y_1, y_2, y_3, \ldots, y_p\}$ where the y_i can be any observation (amplitude, phase, frequency, length, etc.)

b. Feature Extractor

The feature extractor acts on the observations to extract potentially useful information to be used by the classifier.

This can be represented mathematically by Equation (B-1) which maps the observation vector, $\bar{y}$, into the feature vector, $\bar{x}$, through the transformation, T.

$$\bar{X} = T\ (\bar{y}) \qquad \text{(B-1)}$$

c. Classifier

The classifier is used to partition the feature space into decision regions and classify each feature vector, $\bar{x}$, corresponding to a set of observations as belonging to a particular class of objects (w_i). This can be thought of as another mapping, this time from the feature space, X, to the class space, C, which is a discrete space with each point representing a particular class.

The power of the classifier model is that given a set of observations, certain knowledge of the sample statistics (either calculated, measured, or assumed) and a feature extraction procedure, the model can describe the statistical discriminatory ability of a system. The model can be used to optimize the feature extraction process when the features have not already been determined by the type of transducer. The classifier can be used to evaluate existing systems for performance under novel conditions.

3. THE CLASSIFIER MODEL

a. Transducer

The design of the transducer is primarily a function of the particular discrimination problem and the technology available. There is currently no general theory able to determine which observables should be chosen, but the choice can be influenced by certain heuristic insights into the feature extractor. The efficiency of both the feature extractor and classifier is ultimately determined by the quality of observations made by the transducer.

For example, examine a two-color IR system. The transducer comprises the detectors for each of the two-color bands. The detectors sense the IR radiation in each band and convert it to some form of electrical signal, i.e., a machine-usable voltage.

b. Feature Extractor

There are three criteria for the optimum performance of a feature extractor: maximum separability of classes in feature space, minimum loss of discrimination information, and maximum reduction

of data volume. Each of these criteria will carry different priorities according to the problem addressed and the available facilities.

In specifying a two-color system, the feature extraction process has already been defined in that the amplitudes of the signals from each detector are the features which will be used in the discrimination process. In this case, the reduction of data volume has been given maximum priority.

Consider a typical scene from an observation which would be analyzed segment by segment. Each segment can contain either background or target. The output of each detector is a voltage (a_{ix}) proportional to J_i, the incident intensity on the detector. J_i is determined by Equation (A-21) of Appendix A.

Four measurements are made — J_1 and J_2 for both target and background — and recorded for each band in Figure B-2 and plotted in the two-dimensional feature space in Figure B-3.

The measurements map as the two points, (a_{1T}, a_{2T}) and (a_{1B}, a_{2B}) respectively (Figure B-3), and would correspond to the actual "signatures" of each class if the intensities in each color band (J_1, J_2) were uniquely determined and perfectly measured. In this case, the discrimination system would be able to say "If feature f(x,y) = (a_{1T}, a_{2T}), this is a target. If f(x,y) = (a_{1B}, a_{2B}), this is background." However, if a large number of readings are taken (training samples), the points measured will be scattered due to errors in measurements as well as random variations in such target and background properties as temperature, emissivity, area, range, atmospheric conditions, illumination and reflectance, etc. If the number of samples with measured amplitude, a, is plotted versus a, there will be some statistical distribution of the measurements in each band as shown in Figure B-4 (for the one-dimensional case shown for J_1 only).

Thus, the feature space would appear as in Figure B-5 with each class of objects (target and background) described by a distribution of points. In order to differentiate between class w_1 (target) and class w_2 (background) the classifier would use the function g(x,y). Figure B-5 says, "If the feature f(x,y) $<$ g(x,y) this is class w_1." Thus, the feature space is divided into two decision regions by the use of the discriminant function, g(x,y) and the decision rule in quotes which could be denoted as d(x,y,g).

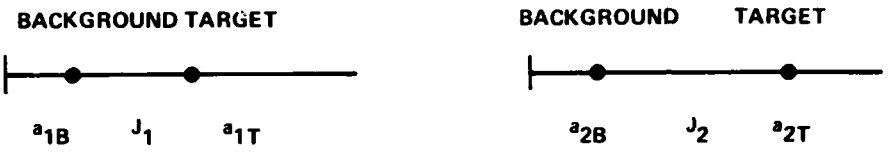

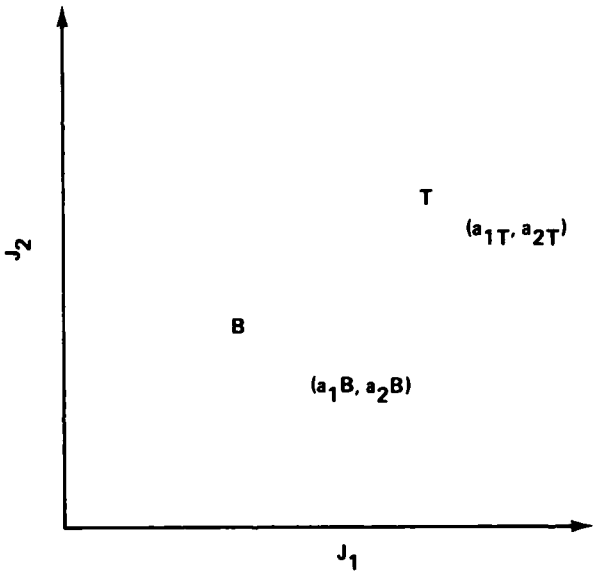

Figure B-3. Two-color feature space.

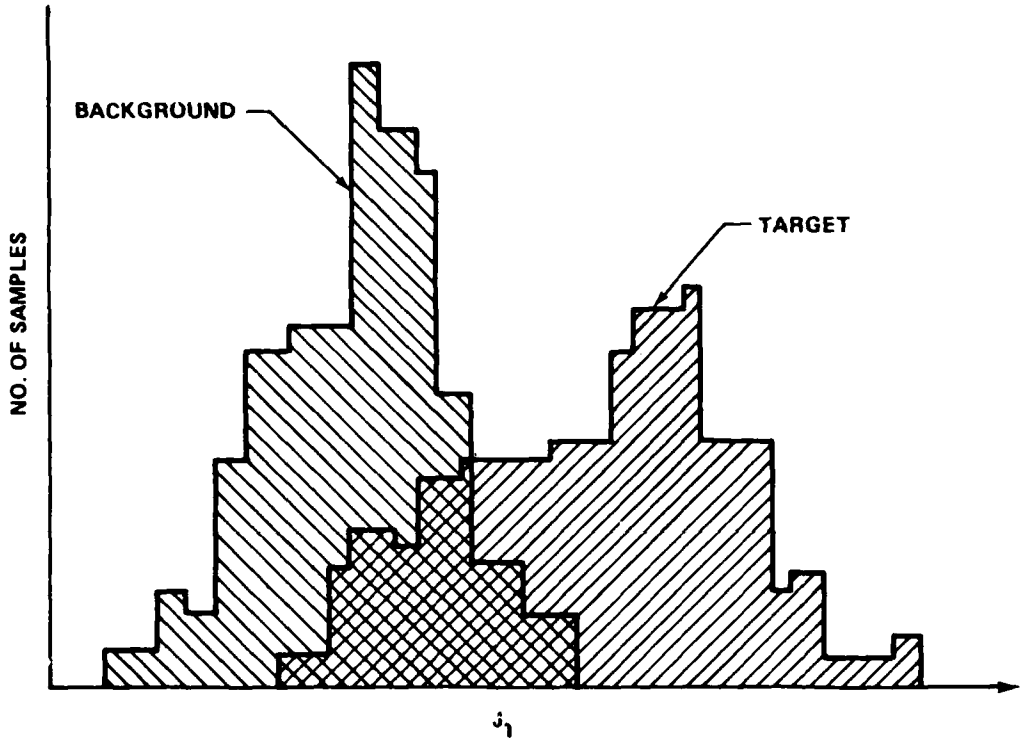

Figure B-4. Statistical distributions of J_1 measurements.

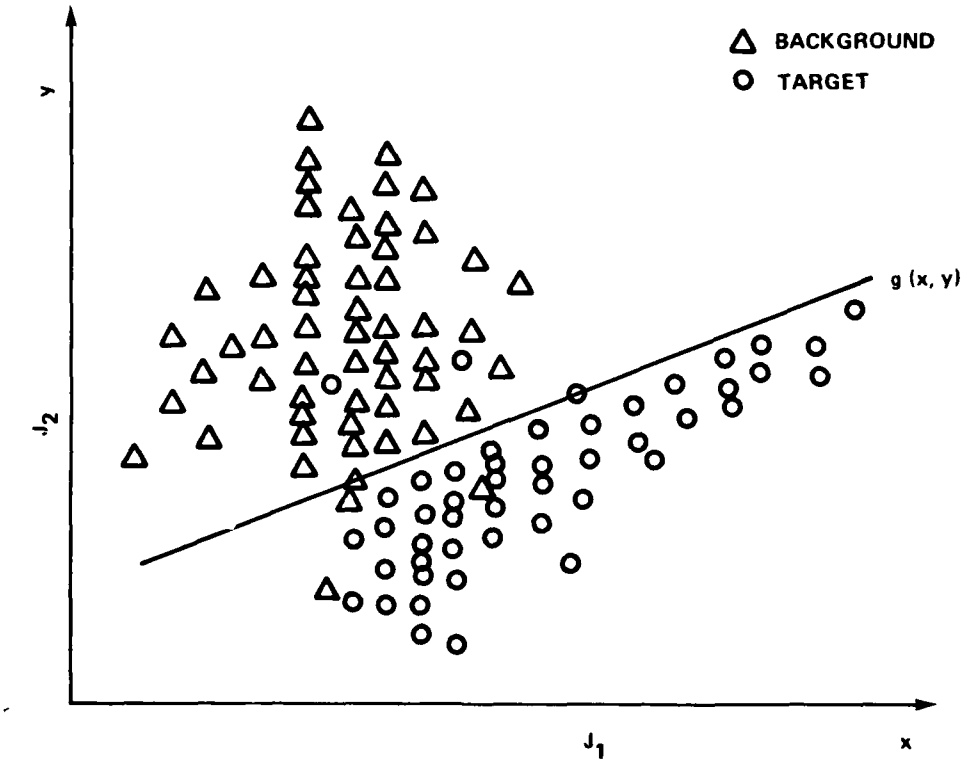

Figure B-5. Two-color feature space with linear discriminant function g(x,y).

A few points of Class w_2 lie in the decision region for Class w_1 and vice versa; hence the discriminant would make an error when classifying these observations. The probability of such an occurrence is defined as the probable error, P(error). To determine the probable error, there must be some knowledge (measured, assumed, estimated, or theoretically derived) of the sample statistics. That is, how are the measurements (real or simulated) scattered by the random variations of the objects and the errors in sensing them?

Much statistical work has been done which indicates that most natural phenomena may be adequately described by a mean vector with a normal distribution of points around it. In three-space, a normal distribution resembles an ellipsoid about the mean (Figure B-6). Thus, if an ellipsoid were to be described in three-space, the mean, direction, and length of the semi-minor and major axes need to be calculated. This may be done in three-space and extended into n-space by the calculation of the variance of the data from the mean. The variance denoted by σ^2 is a measure of the elongation of the data in a particular direction and may be calculated by standard statistical methods. An intuitive feeling for σ is found by the following example. In 95% of the cases considered, a random data value x will fall in the region defined by $|x - \mu| \leq 2\sigma$ where μ is the mean value. Figure B-7 shows the region for one dimension; σ may be considered to be a difference in spectral response in one channel from the mean value. This may be extended to N channels of data by considering that there is a variance associated with each channel of data. Because randomly distributed data within a normal distribution are being used, the values for the mean and the variance associated with a particular class can only be estimated. In general, if a large number of samples are considered to calculate the mean value, the mean will approximate the true mean. If only a small number is considered, there may be significant error in the calculation of the mean for a particular class. In multivariate analysis, the variances in each of the spectral regions are not the only considerations. If data values in some channels depend on data values in other channels, there will be a covariance between the two channels of data. For N channels, this may be represented in an N by N matrix (the covariance matrix). If there is no interdependence, the channels are said to be independent and the covariance is zero. The best estimate for the mean, .., and covariance matrix, Σ, is given as follows:

$$.. = \frac{1}{M} \sum_{k=1}^{M} \overline{X}_k \qquad \text{(B-2)}$$

where X_k is the N-dimensional data vector for the k^{th} training sample and M is total number of training samples,

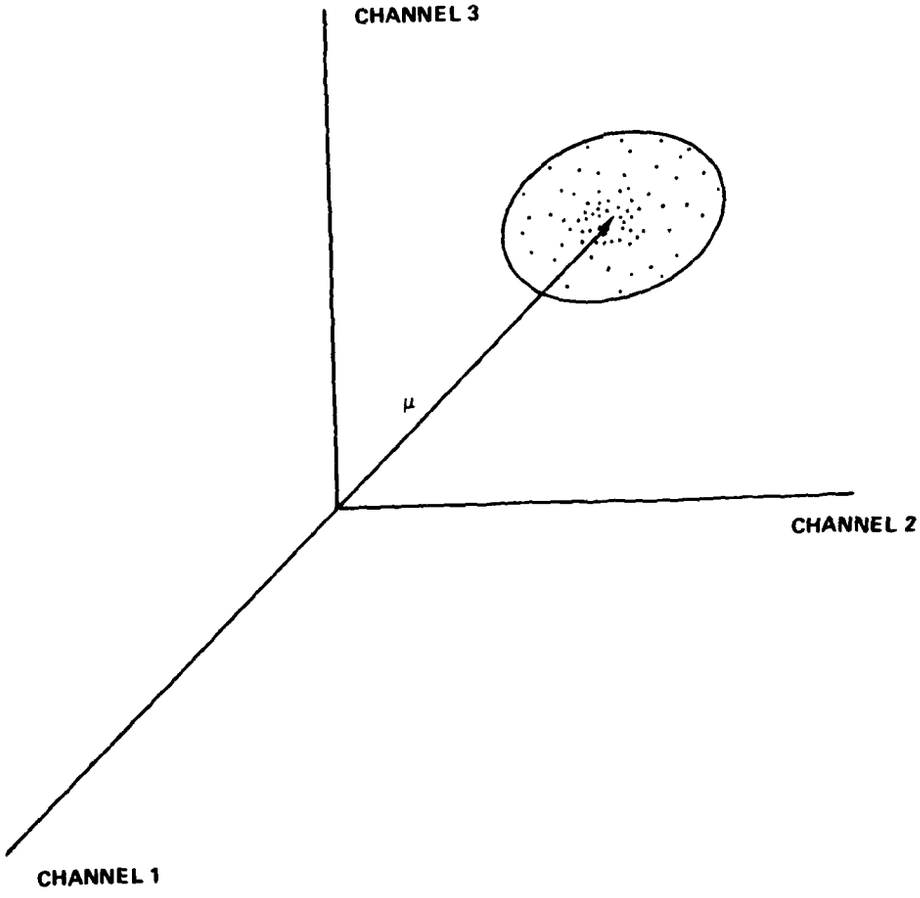

Figure B-6. A three-dimensional feature space.

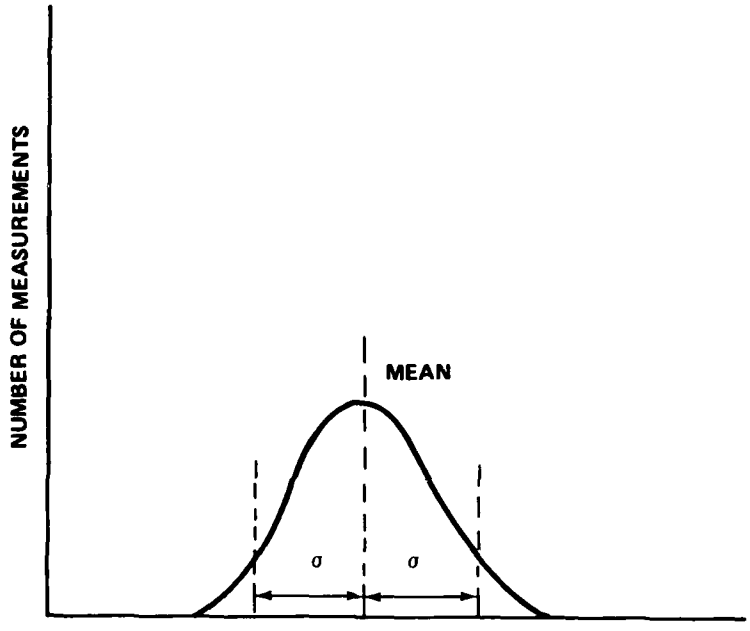

Figure B-7. One-dimensional sample distribution (Gaussian).

$$\sum = \frac{1}{M} \sum_{k=1}^{M} (\bar{X}_k - \mu)\ (\bar{X}_k - \mu)^t \qquad \text{(B-3)}$$

where t indicates that the second matrix is transposed. If a sufficient number of samples are used to define the preceding population or the variances are well-defined, the diagonal elements of the covariance matrix will be the variances squared for each channel and the off-diagonal elements describe the interreaction between channels of data. A sample case for three channels is shown as follows:

$$\hat{\sum} = \begin{vmatrix} \sigma_1^2 & \sigma_1\sigma_2 & \sigma_1\sigma_3 \\ \sigma_2\sigma_1 & \sigma_2^2 & \sigma_2\sigma_3 \\ \sigma_3\sigma_1 & \sigma_3\sigma_2 & \sigma_3^2 \end{vmatrix} \qquad \text{(B-4)}$$

If the channels of data were independent then

$$\hat{\sum} = \begin{vmatrix} \sigma_1^2 & 0 & 0 \\ 0 & \sigma_2^2 & 0 \\ 0 & 0 & \sigma_3^2 \end{vmatrix} \qquad \text{(B-5)}$$

Returning to the feature extraction processes, there are two approaches to optimizing feature extraction: heuristic and statistical.

The heuristic approach tries to extremitize a criterion function, q, which may not be monotonically related to the probability of error. Such methods generally fall into two categories: indirect, which defines a q and tries to optimize it by proper choice of the transformation T; and direct, in which nonmutual properties of each class compose the feature space.

An example of an indirect approach is the Fisher mapping (Figure B-8), which establishes the following criterion function taking into account both interclass and intraclass separations for any two classes by maximizing the distance between sample means while also minimizing the class dispersion.

The criterion function

$$q(w_1, w_2, T) = T(\mu_1 - \mu_2)^2 / T(\Sigma_1 + \Sigma_2)T^t \qquad \text{(B-6)}$$

is maximized for

$$T = (\mu_1 - \mu_2)^t (\Sigma_1 + \Sigma_2)^{-1} \qquad \text{(B-7)}$$

where

μ_i is the statistical mean and gives a measure of interclass separation

N_i is the number of training samples

Σ_i is the covariance matrix and gives a measure of intraclass separation.

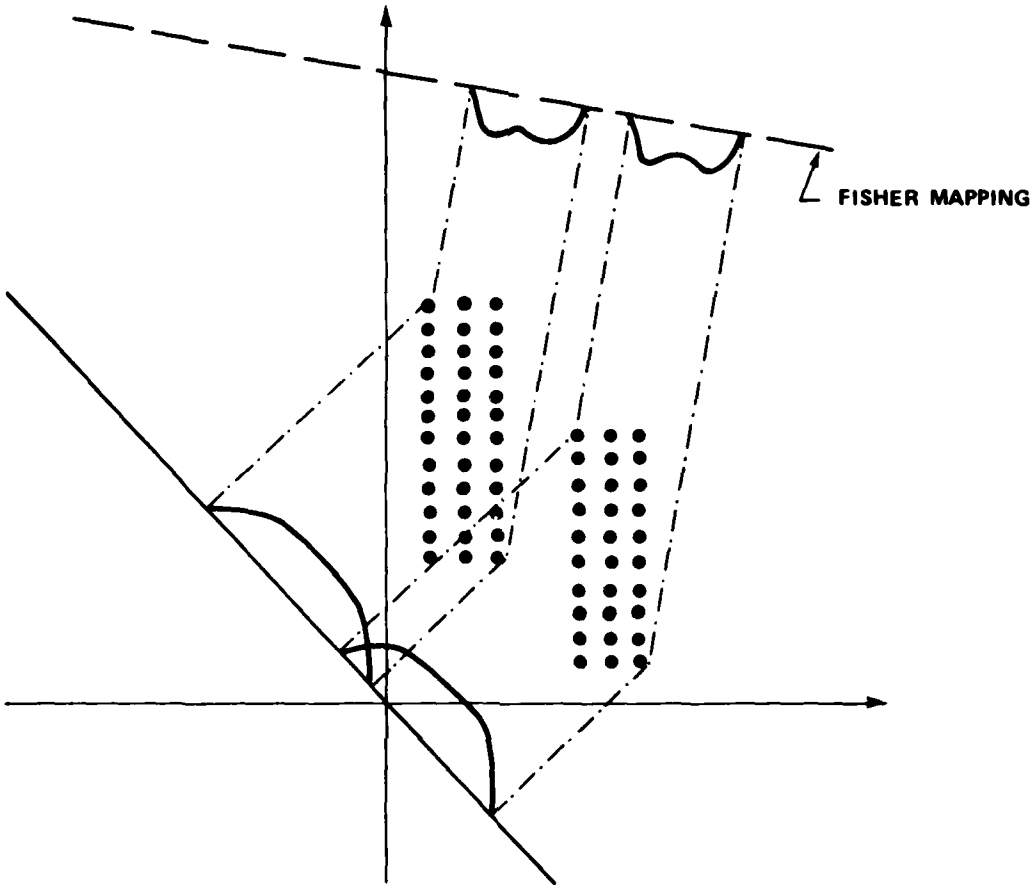

Figure B-8. Fisher mapping.

and the superscripts t and -1 indicate the matrix transpose and inverse, respectively.

The direct approach tries to characterize each class by a set of observations, then select those features which are not shared by both classes. The most common method used is some form of the Karhenun-Loeve transform which orders the importance of the features and thus provides the best characterization of the observations in the mean-square sense while it decorrelates the observations.

The matrix of observations can be thought of as a quadratic surface (usually an ellipse, ellipsoid, or n-dimensional hyper-ellipsoid) with a set of principal axes $\vec{v} = \{v_1, v_2, \ldots, v_i\}$ and a set of reference axes $\vec{u} = \{u_1, u_2, \ldots, u_i\}$ (not necessarily ortho-normal). Similarly, the covariance matrix , which determines the shape of the scattering

of data points, has set, principal axes which are the eigenvectors of , with lengths given by the corresponding eigenvalues. The observation space is transformed so that its principal axes ($\bar{u}_k$) are aligned with those of the covariance matrix. The transformed vectors $\bar{u}_k$ are arranged in descending order of their corresponding eigenvalues. If there are originally N dimensions which are to be reduced to $n \leq N$ dimensions, the mean square error due to the reduction is minimized by taking the first n vectors beginning with the vector with the largest eigenvalue.

An example of the K-L transformation is the subspace method described by Watanabe et al. in which each class is characterized by aligning the axes of the observation space matrix with the axes of the covariance matrix. The representation of the class is given by the axes with the largest components in the transformed space. The feature space (shaded area of Figure B-9) is then taken as the union of the class subspaces minus their intersection(s).

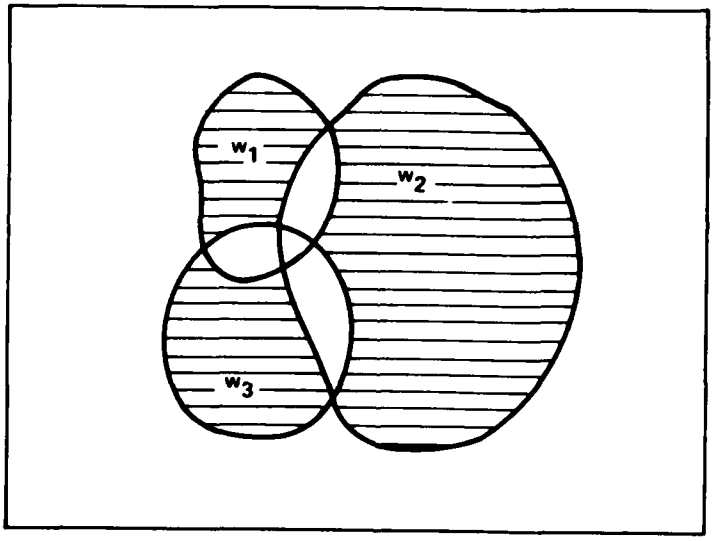

Figure B-9. Subspace method for feature selection.

The statistical approach tries to maximize the separation of classes in feature space. Two "measures" of interclass separation are Jeffrey's Divergence,

$$D = \int_y (p(y|w_1) - p(y|w_2) \ \ell n \left\{ \frac{p(y|w_1)}{p(y|w_2)} \right\} dy \quad , \qquad \text{(B-8)}$$

which is useful for Gaussian distributions as D is the directly related to P(error), and the Bhattacharyya Distance,

$$B = \ell n \int_y \left[p(y|w_1)\ p(y|w_2)\right]^{1/2} dy \quad , \tag{B-9}$$

which bounds the probability of error by the equation

$$P(\text{error}) \leq \sqrt{P(w_1)P(w_2)}\ \exp(-B) \quad . \tag{B-10}$$

The notation for different kinds of probabilities are categorized as follows:

P(x) = probability mass function for discrete random variable x

where $P(a \leq x \leq b) = \int_a^b p(x)\, dx$, defines the probability that x has a value between a and b, where p(x) = probability density function for continuous random variables. P(x, y) is the joint probability distribution which is the probability of an event with values x and y. P(x|y) is the conditional probability density, the probability of an event having value x, given that y is true.

c. Classifier

Once the feature transformation has been selected, the classifier is employed to partition the feature space into decision regions (Figure B-7). Each region is determined by the decision function (alternately called the discriminant function) which can be optimized according to a host of different criteria. For the purposes of target-background discrimination, the most intuitively satisfying measure of classifier performance is determination of expected loss or risk.

The expected loss can be minimized using the Bayes' criterion for the decision rule, d(x) (Figure B-10):

$$d(x) = \begin{cases} x \text{ is in } w_1 \text{ if } g(x) = (b_1)\ p(x|w_1)P(w_1) - (b_2)\ p(x|w_2)P(w_2) > 0 \\ x \text{ is in } w_2 \text{ otherwise.} \end{cases} \tag{B-11}$$

where

$$b_1 = \lambda_{21} - \lambda_{11},\ b_2 = \lambda_{12} - \lambda_{22}$$

λ_{ij} = the loss associated with classifying x as being in w_i when the true state is w_j.

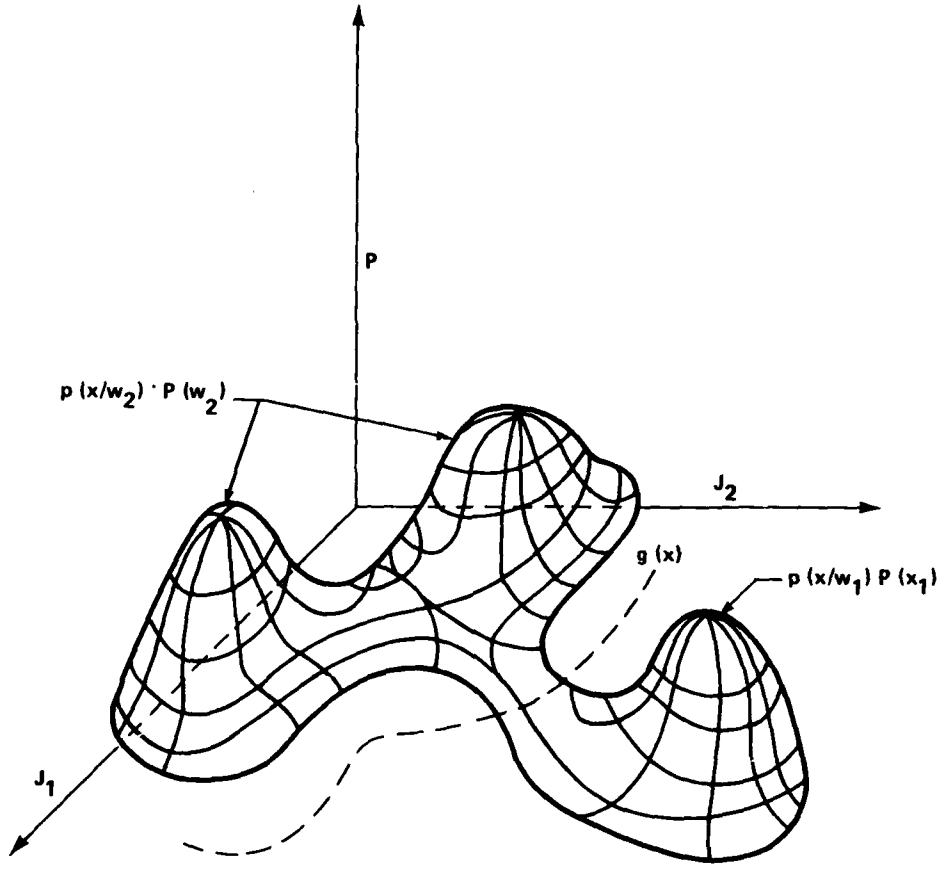

Figure B-10. Bivariate distribution in feature space.

The basis of the Bayes' criterion is that the a posteriori probabilities $P(w_i|x)$ can be calculated from the a priori probabilities $P(w_i)$ and class-conditional probability densities $p(x|w_i)$. The philosophy of Bayesian classification is that these a priori probabilities can be calculated, approximated, assumed, or measured from a set of "training samples" and that this information, although not rigorously supported, is still useful and should be incorporated in the classification process.

Because the normal density function is very often used to represent reality, the discriminant function for it has been known for some time. The discriminant function for a radiance vector $\bar{X}$ to be in the class w_i is

$$g_i(\bar{X}) = -1/2\ (\bar{X} - \bar{\mu})^t \Sigma_i^{-1}\ (\bar{X} - \bar{\mu}) - \frac{N}{2} \log 2\pi$$

$$-1/2 \log |\Sigma_i| + \log P(w_i) \qquad \text{(B-12)}$$

where $\bar{\mu}$ is the mean vector and Σ_i^{-1} is the inverse of the i^{th} class covariance matrix. In general, the $\frac{d}{2} \log 2\pi$ term is only additive and is not a function of which class is considered. Thus it may be ignored. By replacing $g_i(x)$ by $f(g_i(\bar{X}))$ where f is a monotonically increasing function, the resulting classification is unchanged. Thus, if the exponential of $g_i(\bar{X})$ is taken, a new discriminant function is found:

$$Q_i = f(g_i(\bar{X}) = \frac{e^{-1/2(\bar{X} - \bar{\mu})^t \Sigma_i^{-1} (\bar{X} - \bar{\mu})}}{|\Sigma|_i^{1/2}} \quad . \qquad \text{(B-13)}$$

Now for every radiance vector $\bar{X}$, a Q is calculated for each class previously defined. The vector is then assigned to the class that has the largest value of the discriminant function Q. This proceeds until all the radiance vectors for the imaged area are processed. One pitfall of this method is that a vector is always assigned to one of the classes even though it actually may not be similar to any of the classes.

Because the $|\Sigma_i|^{1/2}$ and the Σ_i^{-1} need only be calculated once for each class, the most time-consuming part of the calculation for each data vector is the quadratic computation of $(\bar{X} - \bar{\mu})^t \Sigma_i^{-1} (\bar{X} - \bar{\mu})$.

Thus this method uses statistics generated by a large number of samples to describe each class of data to which a vector may be assigned. The discriminant function must be calculated for each class for every data vector which is then assigned to one of those classes by inspection of the discriminant functions.

The Bayes' criterion therefore requires some knowledge of the <u>a priori</u> probabilities $P(w_i)$ corresponding to the probabilities of occurrence of each Class w_i. The Neyman-Pearson criterion avoids this requirement (but pays the price with additional analytical complexity) by minimizing the risk of Class w_2 while keeping the risk of Class w_1 constant.

For a zero-one loss function (that is, any error has a weight one and any correct decision has zero penalty), the criterion function is minimized

$$q(d) = P(\text{error}|w_2) \tag{B-14}$$

while $P(\text{error}|\ w_1) \leq \epsilon_o$

which is minimized for the decision rule,

$$d(x) = \begin{cases} w_1 \text{ if } p(x|w_1)/p(x|w_2) > \mu \\ \\ w_2 \text{ otherwise} \end{cases} \tag{B-15}$$

where μ is found by

$$\epsilon_o = \int_{\mu}^{\infty} p(\ell|w_1)\ d\ell \tag{B-16}$$

and $p(\ell|w_1)$ is the class conditional probability density of the likelihood ratio

$$\ell \equiv p(x|w_1/p(x|w_2) \quad . \tag{B-17}$$

Nearly all classification methods require some knowledge about the statistics of the intended discriminant classes. Unless an analytic model for all the classes can be constructed, these statistics must be inferred from a set of "training samples."

The sample statistics can be approximated using parametric methods to fit sample measurements to some assumed distribution (such as a Gausian or normal distribution) which is then used as the analytic distribution. Nonparametric methods use known relations in the data to construct density estimates which hopefully converge to the true probability densities. Examples of such methods are Parzen-type and k-th nearest neighbor estimates.

Once the statistical properties for the problem at hand have been determined, the classifier is evaluated for probability of error during performance. Two courses of action are available for the design of the classifier as follows:

1) The training samples employed for the classifier design are used for the evaluation of the classifier. This generally results in an optimistic (best-case) estimate of classifier performance.

2) An evaluation set of samples which are different from the training set are used. This gives a pessimistic (worst-case) evaluation of the classifier.

REFERENCES

1. Lawson, W. R., and Katches, J. A., "Thermal Imaging Systems Models," Proc. of IRIS Speciality Group on Imaging, November 1972.

2. Bracewell, R., The Fourier Transform and its Application, New York: McGraw-Hill, 1965.

3. Zajac, H., Optics, New York: Addision-Wesley, 1974.

4. Hudson, R. Jr., Infrared Systems Engineering, New York: John Wiley and Sons, 1969.

5. Papoulis, A., Probability, Random Variables, and Stochastic Processes, New York: McGraw-Hill, 1965.

6. Stein, S., Modern Communication Principles, New York: McGraw-Hill, 1967.

7. Seyrafi, K., "Electro-Optical Systems Analysis," Electro-Optical Research Company, 1977.

8. Lloyd, J. M., Thermal Imaging Systems, New York: Plenum Press, 1975.

DISTRIBUTION

	No. of Copies
Defense Documentation Center Cameron Station Alexandria, Virginia 23144	12
Commander US Army Materiel and Readiness Command Attn: DRCRD DRCDL 5001 Eisenhower Avenue Alexandria, Virginia 22333	 1 1
Superior Technical Services, Inc. 4308 Governors Drive Attn: T. Ward Huntsville, Alabama 35805	 1
DRSMI-FR, Mr. Strickland -LP, Mr. Voigt	1 1
DRDMI-X, Dr. McDaniel -T, Dr. Kobler -TE, -TB -TI (Record Set) (Reference Copy)	1 1 13 3 1 1